Preprints.org

Review

Unraveling Peritoneal Carcinomatosis on Cross-Sectional Imaging Modalities

Ana Veron Sanchez [*] , Ilias Bennouna , Nicolas Coquelet , Jorge Cabo Bolado , Inmaculada Pinilla Fernandez , Luis Alberto Mullor Delgado , Martina Pezzullo , Gabriel Liberale , Maria Gomez Galdon , Maria Antonietta Bali

Review

Unraveling Peritoneal Carcinomatosis on Cross-Sectional Imaging Modalities

Ana Veron Sanchez [1],*, Ilias Bennouna [1], Nicolas Coquelet [1], Jorge Cabo Bolado [2], Inmaculada Pinilla Fernandez [3], Luis A. Mullor Delgado [4], Martina Pezzullo [5], Gabriel Liberale [1], Maria Gomez Galdon[1] and Maria A. Bali [1]

[1] Ana Veron Sanchez. Hôpital Universitaire de Bruxelles, Institut Jules Bordet, Brussels, Belgium, ana.veron@hubruxelles.be, Ilias Bennouna ilias.bennouna@hubruxelles.be, Nicolas Coquelet nicolas.coquelet@hubruxelles.be, Gabriel Liberale gabriel.liberale@hubruxelles.be, Maria Gomez Galdon maria.gomezgaldon@hubruxelles.be,   Maria A. Bali maria.bali@hubruxelles.be

[2] Jorge Cabo Bolado. Teleconsult, Milton Keynes, Buckinghamshire, England, jorgecabobolado@gmail.com

[3] Inmaculada Pinilla Fernandez, Hospital Universitario La Paz, Madrid, Spain, minmaculada.pinilla@salud.madrid.org

[4] Luis A. Mullor Delgado. Hospital Universitario Gregorio Marañon, Madrid, Spain, luisalberto.mullor@salud.madrid.org

[5] Martina Pezzullo. Hôpital Universitaire de Bruxelles, Hôpital Erasme, Brussels, Belgium, martina.pezzullo@hubruxelles.be

* Correspondence: ana.veron@hubruxelles.be

Abstract: Peritoneal carcinomatosis (PC) refers to malignant epithelial cells spread to the peritoneum, principally from abdominal malignancies. Until recently, PC prognosis has been considered ill-fated, with palliative therapies as the only treatment option. New loco-regional treatments are changing the outcome of PC and imaging modalities have a critical role for early diagnosis and disease staging, determining treatment decision-making strategies. Among cross-sectional imaging modalities, computed tomography (CT) is more available and faster; however, magnetic resonance (MR) performs better in terms of sensitivity and specificity, due to its higher contrast resolution. The appearance of peritoneal deposits on CT and MR depends mainly on the primary tumour histology: in case of unknown primary tumour (3-5% of cases), their behaviour at imaging may provide insights on the tumour origin. The time-point of tumour evolution, previous or ongoing treatments and the peritoneal spaces where they occur, also play an important role in determining the appearance of peritoneal deposits. Thus, knowledge of peritoneal anatomy and fluid circulation is mandatory in detection and characterization of peritoneal deposits. Several benign and malignant conditions may show similar imaging features that overlap those of PC, making the differential diagnosis challenging.   Clinical history, laboratory findings and previous imaging examinations must be considered to achieve the correct diagnosis.

Keywords: peritoneum; carcinomatosis; deposits

1. Introduction

The peritoneum is the second most common metastatic location for abdominal tumours, only surpassed by the liver.

As a matter of fact, only 10% of the cases of peritoneal carcinomatosis (PC) are related to extra abdominal tumours [1], being breast (41%), lung cancers (21%) and malignant melanoma (9%) the most frequent causes [2].

Traditionally, PC implied an ill-fated prognosis and only palliative treatments were applied. However, the introduction of new surgical techniques and regional therapies have changed this scenario and palliative systemic treatment is no longer the only therapeutic option.

Thus, despite its difficulty, early diagnosis of PC based on imaging findings is essential for disease staging, for the subsequent management of primary tumours and for patient prognosis.

2. Diagnostic Modalities

The gold standard for the assessment of PC is explorative laparoscopy. However, as an initial approach, cross-sectional imaging modalities are preferred and the most common and widespread imaging technique used is intravenous contrast-enhanced (CE) Computed tomography (CT) thanks to its availability, fast acquisition time and the possibility of multiplanar reconstructions [3,4]. The administration of water density oral contrast may improve the detection of peritoneal deposits, especially those adjacent to the bowel [5]. CE CT has demonstrated a 68% sensitivity and 88% specificity for the detection of peritoneal deposits, although their size and location can undermine this performance [4,6].

Magnetic resonance (MR) including diffusion weighted imaging (DWI) and contrast enhanced T1-weighted sequences is a promising diagnostic modality as it provides higher sensitivity (91%) and specificity (85%) compared to CE-CT [5] due to its high contrast resolution, which allows to distinguish tumour from surrounding non tumour tissues. Moreover, in the presence of moderate to substantial ascites, MR still performs better than CT [7].

A third non-invasive imaging modality available to assess peritoneal carcinomatosis is PET-CT (Positron emission tomography fused with CT images), which provides metabolic information of the lesions, based on the measurement of the increased uptake of a radiotracer, mostly a glucose analog: FDG ([18F]-2-deoxy-2-fluoro-D-glucose. It improves the diagnostic performance of CT but shows slightly lower sensitivity (87%) than MR, probably due to its lower spatial resolution with limited depiction of small nodules. On the other hand, its specificity is slightly higher (92%) [8]. Moreover, FDG-PET-CT provides a whole-body assessment, which is a major advantage in detecting extra-abdominal metastases. However, besides the high costs, PET-CT is less available, and it may provide false negative findings, as for mucinous tumours [4] and false positive findings, as for postoperative abnormalities, infectious or inflammatory conditions.

3. The Many Places and the Many Faces

The term peritoneal carcinomatosis (PC) refers to a spread of malignant epithelial cells as tumour deposits to the peritoneum {9}.

PC represents a very complex condition at imaging, more than any other metastatic site.

The appearance of the peritoneal deposits is determined not only by the histological characteristics of the primary tumour, the time-point of the tumour-evolution and the treatment [10] but also, and more interestingly, by the peritoneal space where they occur.   Complications secondary to deposits will also vary according to the location, depending on the organs involved.

Some anatomic knowledge will be required in the quest for deposits. The aim of this review is not to cover a comprehensive description of peritoneal anatomy but sufficiently to be sure that all locations will be thoroughly investigated.

The peritoneal cavity is the virtual space that exists between the parietal and visceral peritoneum [11] and in normal conditions, it contains a small amount of plasma-like fluid.

The parietal peritoneum delineates the periphery of the peritoneal cavity:

- Cranially: it covers the diaphragm (except for the bare area of the liver, the insertion of the ligaments and along its posterior margin where it is in contact with the retroperitoneal fat) (Figure 1).
- Caudally: it descends into the pelvis. Its complex anatomy in this location will be seen in detail later.
- Anterolaterally: it is separated from the abdominal wall by the fat from the preperitoneal space, that is, the space between the peritoneum and the transversalis fascia (Figure 2).
- Posteriorly: it is distanced from the posterior abdominal wall by the retroperitoneal space. It forms the anterior boundary of the retroperitoneal space (Figure 3).
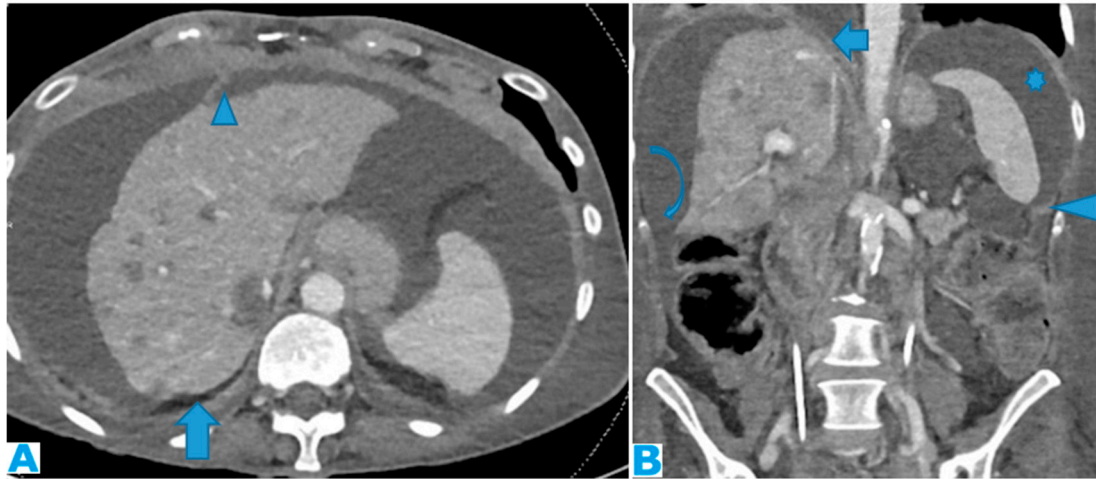
Figure 1. Axial CE-CT (**A**) and coronal MPR (**B**). Massive ascites, helpful to differentiate the peritoneal spaces. Observe on **A** how the posterior margin of the diaphragm (arrow) is not covered by the parietal peritoneum as it is directly in contact with the retroperitoneal fat. The attachment sites of ligaments on the diaphragmatic surface are not covered by peritoneum; Identify on **A** the falciform and on **B**, the phrenicocolic ligaments (arrowhead). Notice on **B** how the phrenicocolic ligament partially separates the left parietocolic gutter from the left subphrenic space (*), whereas the right parietocolic gutter fully communicates with the right subphrenic space (curved arrow). Identify the bare area of the liver on **B** (arrow), an area directly attached to the diaphragm by connective tissue, thus not covered by peritoneum as neither is its diaphragmatic attachment site.
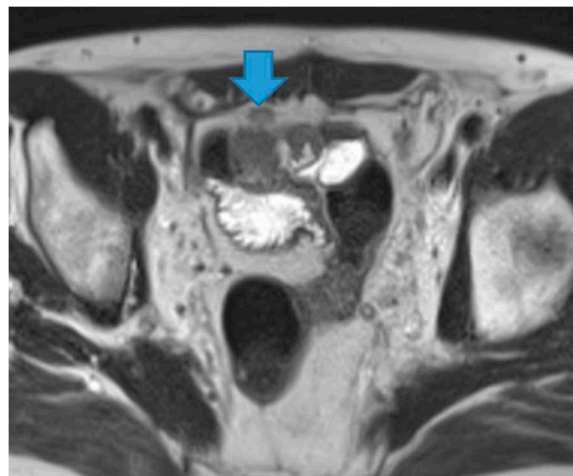

Figure 2. Axial T2WI.PC from neuroendocrine tumour: Deposit within anterior parietal peritoneum.

Preprints (www.preprints.org) | NOT PEER-REVIEWED | Posted: 9 May 2023   doi:10.20944/preprints202305.0576.v1
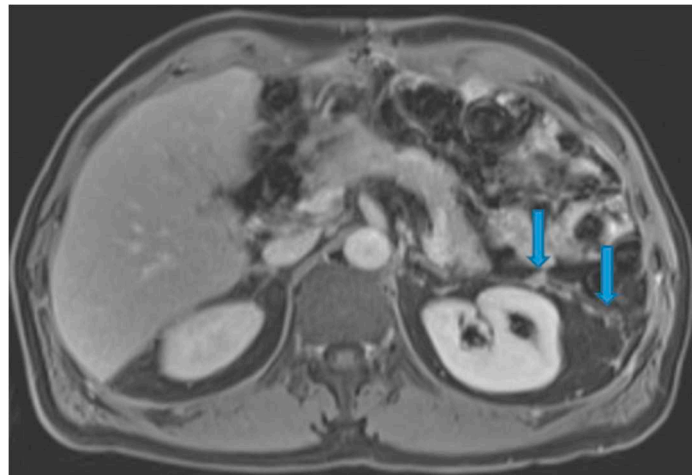
4

Figure 3. Axial T2WI. PC from neuroendocrine tumour: Deposits within the posterior parietal peritoneum (arrows) (which is immediately anterior to the anterior pararenal fascia).

The peritoneum invaginates to fully cover most of the abdominal viscera, anterior and posteriorly, becoming the visceral peritoneum. It is organized into a folded disposition as ligaments, folds, and mesenteries to nurture, innervate and support the intraperitoneal organs, connecting them to the posterior parietal peritoneum.

As a common rule, abnormal thickening and pathological enhancement of surfaces covered by the peritoneum may be the only initial imaging finding in PC.

It may be difficult, in the absence of ascites, to differentiate parietal peritoneal deposits from their visceral counterparts on locations where the two leaves are adjacent (e.g.: a deposit within the parietal peritoneum covering the lateral abdominal wall or within the visceral peritoneum covering the liver). For the sake of simplicity, some examples of parietal peritoneal deposits will be shown now, the rest will be included within their peritoneal space (Figure 4).
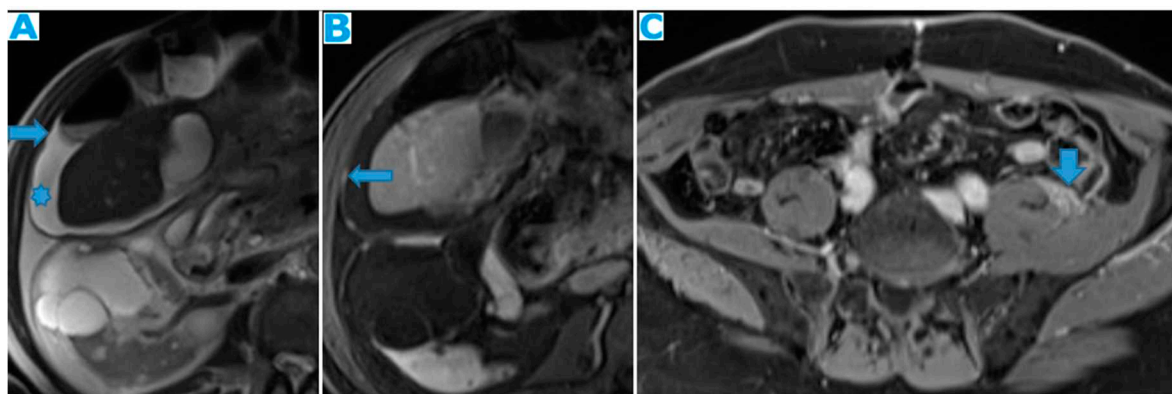

Figure 4. Axial T2WI (**A**), axial CE portal phase FST1WI (**B**), same patient. PC from colon adenocarcinoma: Notice the nodular thickening of the parietal peritoneum due to deposits. Notice how easy it is to distinguish the parietal peritoneum from the visceral perihepatic peritoneum thanks to the ascites (*). Axial CE portal phase FST1WI (**C**). PC from neuroendocrine tumour: Deposit within the posterior parietal peritoneum. The retroperitoneal space is very thin at this location and so the posterior parietal peritoneum is adjacent to the abdominal wall.

If the deposit lies within a fat containing peritoneal space, the spectrum of presentation ranges from nodular focal fat stranding to irregular haziness, evolving towards solid lesions. These solid lesions may be initially millimetric, appearing as either solitary to multiple soft tissue nodules that will eventually grow and merge to form plaques or sheets and then masses. Most commonly, PC appears as a combination of all these findings.

Peritoneal spaces are classified as supra or inframesocolic [12,13].   The anatomic landmark that enables this division is the **mesentery of the transverse colon** (transverse colon mesocolon). Unfortunately, it is also an easy route for carcinomatosis spread as it communicates on both sides with other ligaments and centrally with the small bowel mesentery.

Deposits within the transverse mesocolon will appear either on its mesentery (Figure 5) or /and on the serosa covering the transverse colon [14], and differentiation between them may not always be feasible. Deposits may cause different degrees of luminal stenosis with or without signs of bowel obstruction.
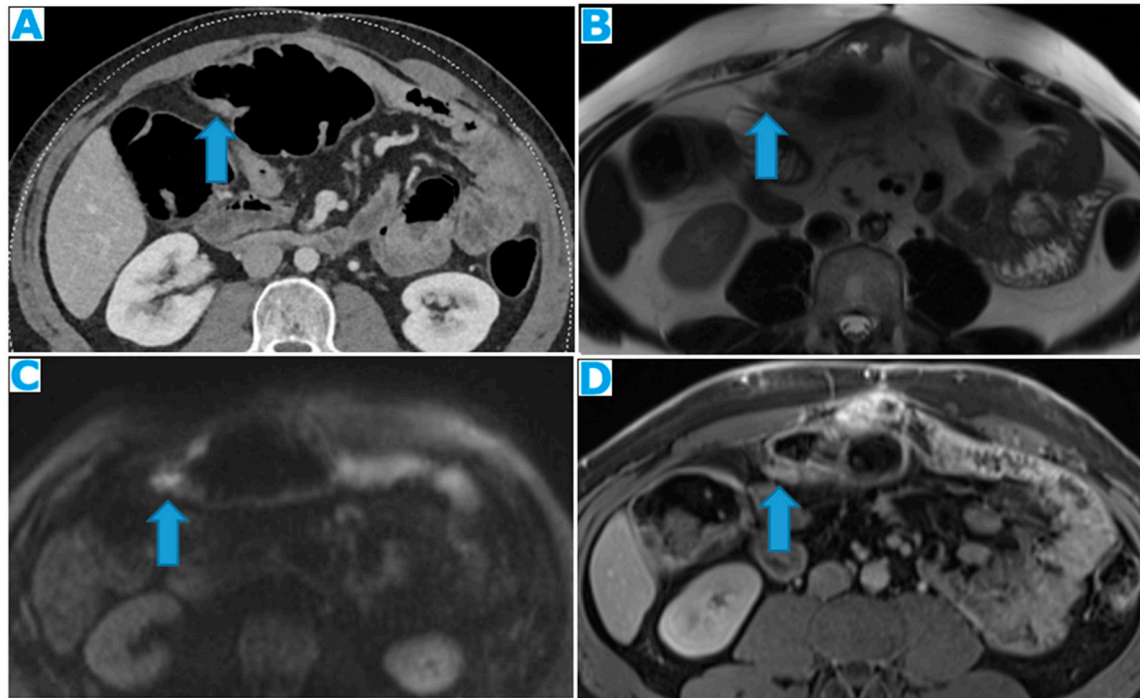

Figure 5. Axial CE-CT (A), axial T2WI (B), DWI (**C**), axial CE portal phase FST1WI (**D**). PC from gastric adenocarcinoma: Subtle deposit within the transverse mesocolon on CT, more conspicuous on MR.

Imaging features of serosal bowel deposits include nodular lesions, segmental parietal thickening, and diffuse infiltration. Their detection may be an arduous task, more so if bowel is not sufficiently distended. In addition, it is important to bear in mind that layered implants will blend in with the bowel contour, whereas nodular deposits will alter it and thus are easier to detect (Figure 6).
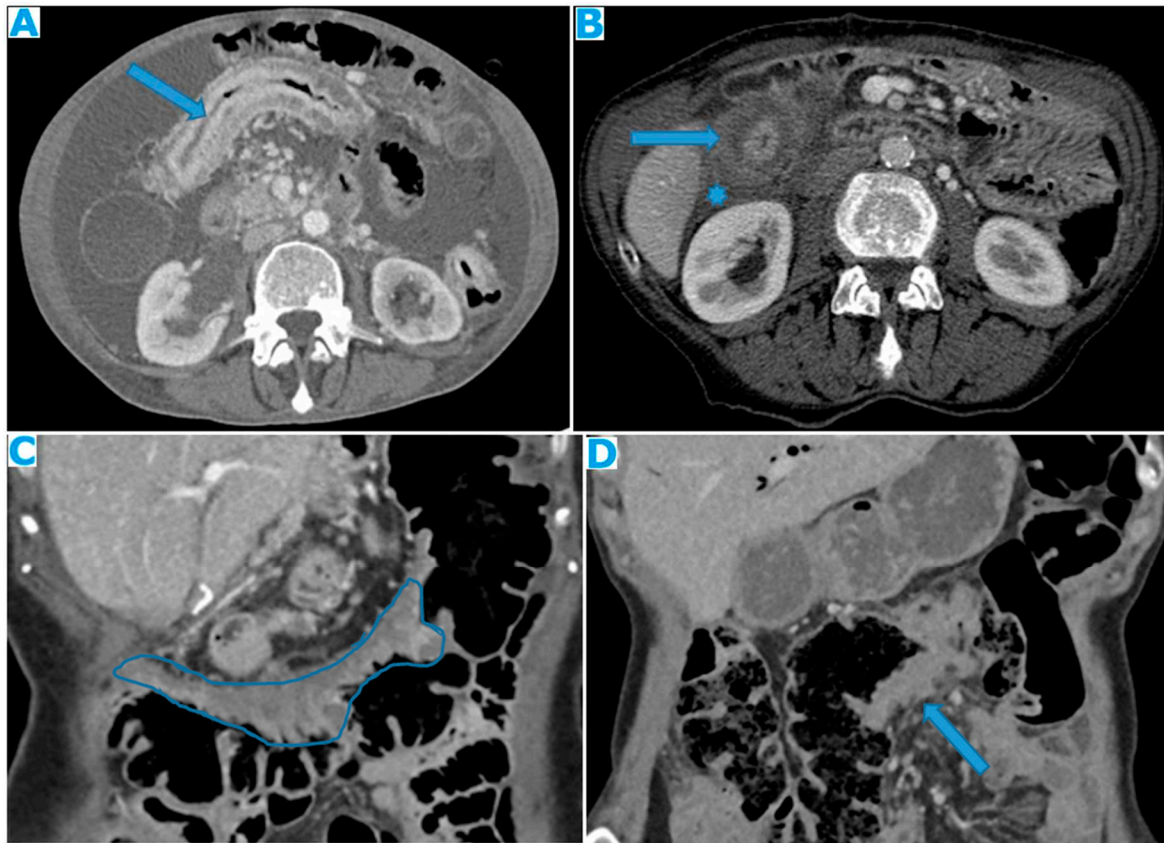
Figure 6. Axial CE-CT (**A**). PC from breast carcinoma: Deposits within the transverse colon serosa (arrows), causing luminal stenosis. Axial CE-CT (**B**). PC from breast carcinoma: Layered deposits within the transverse colon serosa (arrow), notice the concentric pattern and the luminal stenosis. Ascites (*). Coronal CE-CT MPR (**C-D**). **C**: PC from signet ring cell gastric carcinoma. Diffuse serosal infiltration of the transverse colon. **D**: PC from breast carcinoma: Segmental parietal thickening of the transverse colon due to nodular deposits within the serosa (arrow). Observe how layered deposits on **C** blend in with the bowel contour and may be more difficult to detect than nodular deposits on **D**.

This description of serosal bowel deposits has the same validity as for the rest of the gastrointestinal tract.

A cranial-to-caudal and lateral-to-medial approach will be used to review the peritoneal spaces.

3.1. Supramesocolic Spaces

Supramesocolic cavity comprehends the subphrenic, perihepatic and perisplenic spaces, periportal space, lesser omentum, lesser sac and right subhepatic space. These locations need to be carefully assessed using multiplanar reconstructions as deposits within them may require a complex surgery or in some cases may be considered unresectable.

3.1.1. Subphrenic Spaces

Imaging features include thickening and pathological enhancement of the diaphragm, nodules, and masses (Figures 7 and 8).
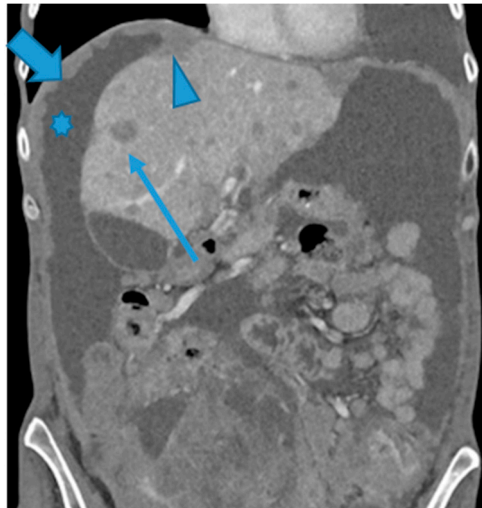
Figure 7. CE-CT coronal MPR. PC from ovarian carcinoma: Multiple bilateral diaphragmatic nodular deposits (arrows). Notice how useful ascites (*) is to distinguish peritoneal deposits within the parietal peritoneum from deposits within the visceral (hepatic) peritoneum (arrowhead). Hepatic metastases (thin arrow).
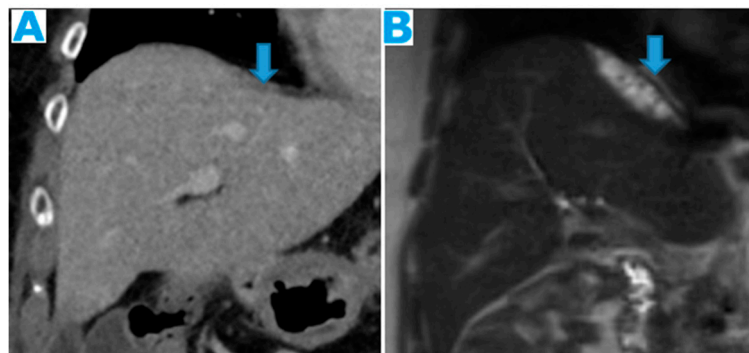

Figure 8. Coronal T2WI (**A**, from five years prior) and CE-CT coronal MPR (**B**, current follow up). PC from ovarian granulosa cell tumour: Notice on **B** a deposit within the right subphrenic space, bulging into the hepatic capsule. See how subtle it originally was on **A**, easily overlooked on axial imaging.

3.1.2. Perihepatic and Perisplenic Spaces

Deposits can be identified as a continuum from abnormal peritoneal enhancement to subtle nodularity and well-defined nodules, often showing a biconvex morphology.

Perihepatic deposits may occur on the superficial visceral peritoneum that surrounds most of the liver surface (except for the liver bare area, the porta hepatis and the attachment site of the gallbladder to the liver) and/or underneath Glisson capsule, within the subcapsular space. Glisson´s capsule is a thick fibrous membrane that lies deep to the visceral peritoneum. It is assumed that deposits infiltrate the liver capsule upon deposition on the visceral peritoneum. Liver capsule covers the entire hepatic surface, including the periportal space, and is in communication with the lesser omentum, thus becoming another route for deposits to reach the subcapsular space.   Both the periportal space and the lesser omentum will be reviewed next.

In the event of subcapsular deposits, secondary parenchymal invasion may occur, resulting in a characteristic scalloping of the underlying parenchyma (Figure 9). Despite this sign, sometimes it may be difficult to distinguish between solely subcapsular deposits and those with parenchymal invasion.   A sign that has been found to be highly sensitive to rule out secondary hepatic invasion is the presence of a well-defined interface between the lesion and the liver and/or a clear plane either fatty or from ascites [15] (Figure 10).
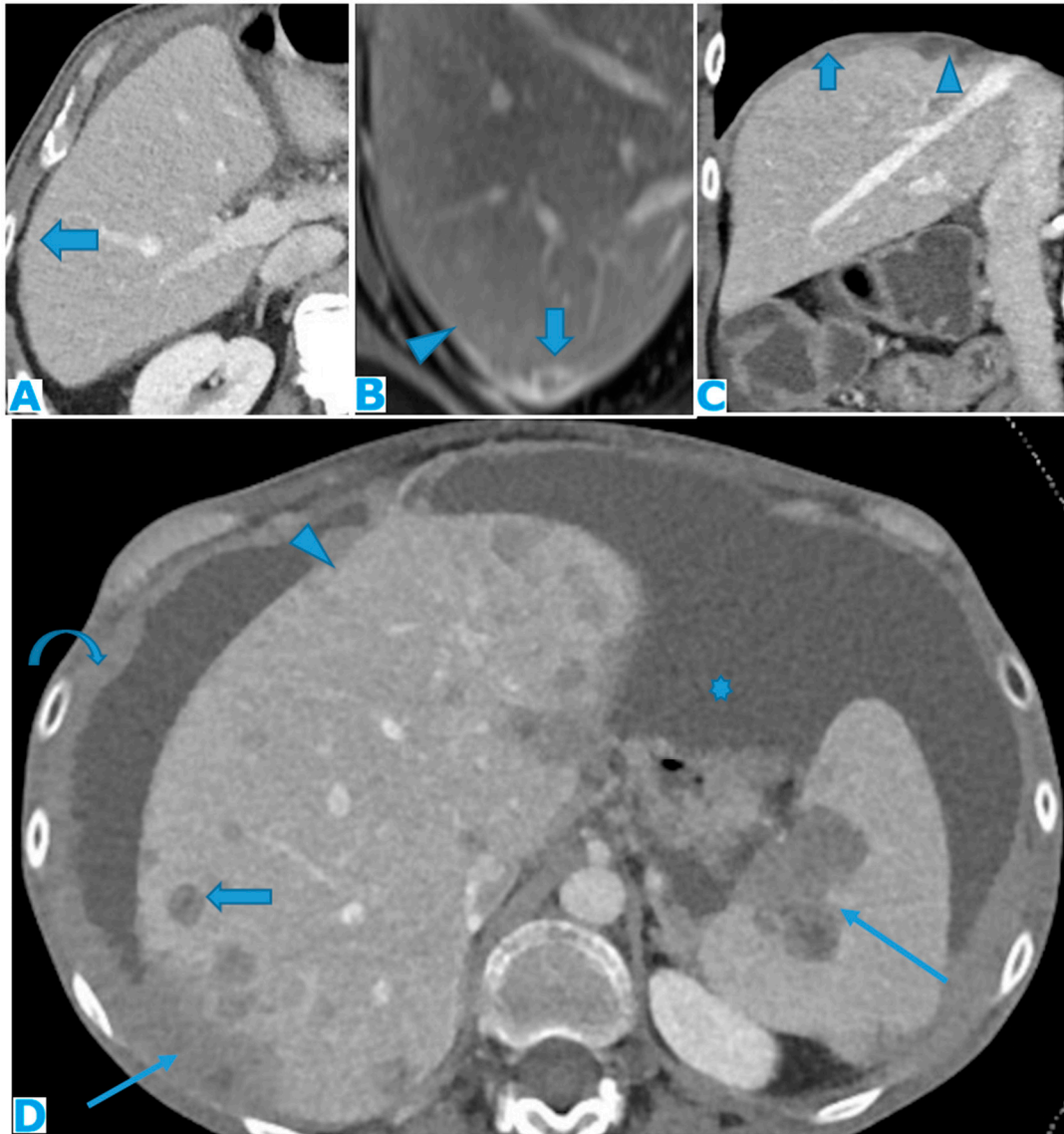
Figure 9. Axial CE-CT (**A**): PC from colon carcinoma: Note the subtle irregularities of the liver contour caused by the deposit seeding within the peritoneum covering the hepatic surface. CE portal phase FST1WI (**B**): PC from cervical carcinoma: Notice the difference between the linear subcapsular deposits (arrowhead) and the biconvex subcapsular deposit with parenchymal invasion (arrow): observe the scalloped appearance of the underlying parenchyma. CE-CT coronal MPR (**C**): PC from colon carcinoma: Thickening of the right diaphragm caused by deposit seeding (arrow). Notice the difference with the subcapsular deposits that scallop the liver contour (arrowhead). Axial CE-CT (**D**): PC from ovarian carcinoma: Subcapsular deposits with parenchymal invasion (thin arrows), both hepatic and splenic. Observe how they differ from hepatic metastases, well defined and completely surrounded by parenchyma (arrow). Note also perihepatic (arrowhead) and right subphrenic deposits (curved arrow). Ascites (*).
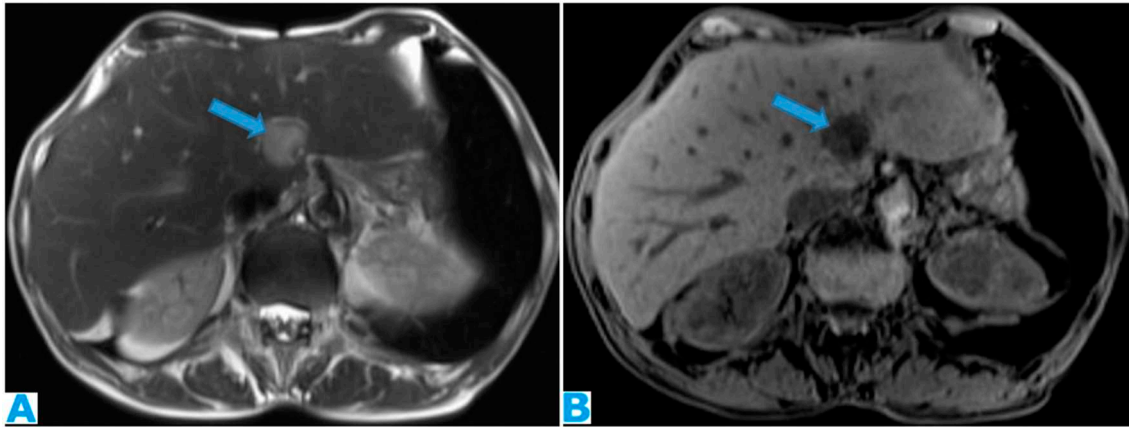
Figure 10. Axial T2WI (**A**), axial NE FST1WI (**B**). PC from ovarian serous carcinoma: Subcapsular hepatic deposit, presenting a fatty plane around (arrow) that excludes secondary hepatic invasion.

3.1.3. Periportal Space

Periportal deposits need to be well differentiated from parenchymal metastases. Deposits within the periportal space will appear as nodular or plaque-like lesions, predominantly at the porta hepatis and along the left branch of the portal vein; they are usually ill defined and not circumferentially surrounded by hepatic parenchyma, unlike their intraparenchymal counterparts (Figure11).
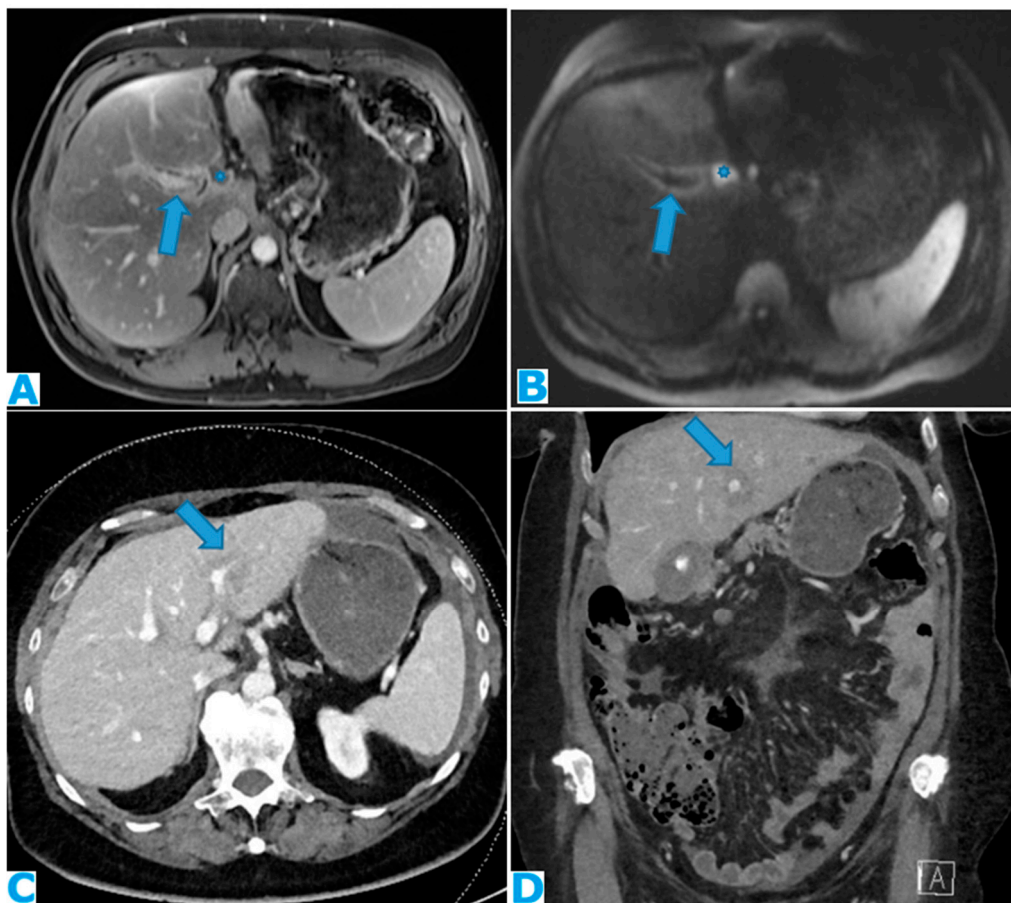

Figure 11. DWI (**A**), axial CE portal phase FST1WI (**B**). PC from colon carcinoma: deposits within the periportal space. Observe the diffusion restriction and enhancement around the periportal space (arrows); also note the nodular deposit (*). Axial CE -CT(**C**) and coronal MPR (**D**). PC from ovarian carcinoma: Note the periportal deposit as a soft tissue mass around the left portal branch, more conspicuous on the MPR.

A proven useful tip is the distention of the periportal space over time due to the presence of deposits. As with any radiological examination, comparison with prior images in the setting of peritoneal carcinomatosis is mandatory (Figure 12).
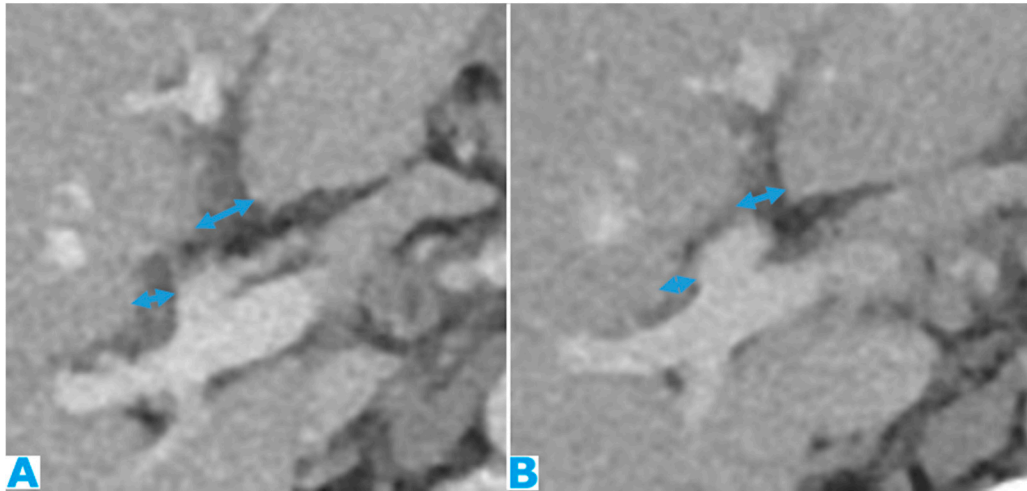

Figure 12. Axial CE-CT (**A**, current study, and **B**, from one year prior). PC from gastric adenocarcinoma: Subtle soft tissue mass occupying the periportal space. Observe the periportal space enlargement, more conspicuous if compared to the previous CT.

Deposits within this location may cause biliary obstruction, which usually presents at a late stage. Dilatation of the intrahepatic biliary ducts (usually segmentary) with no identifiable cause should raise the possibility of deposits within the periportal spaces. Another secondary finding may be a progressive compressive effect on the portal vein over time (Figure13).
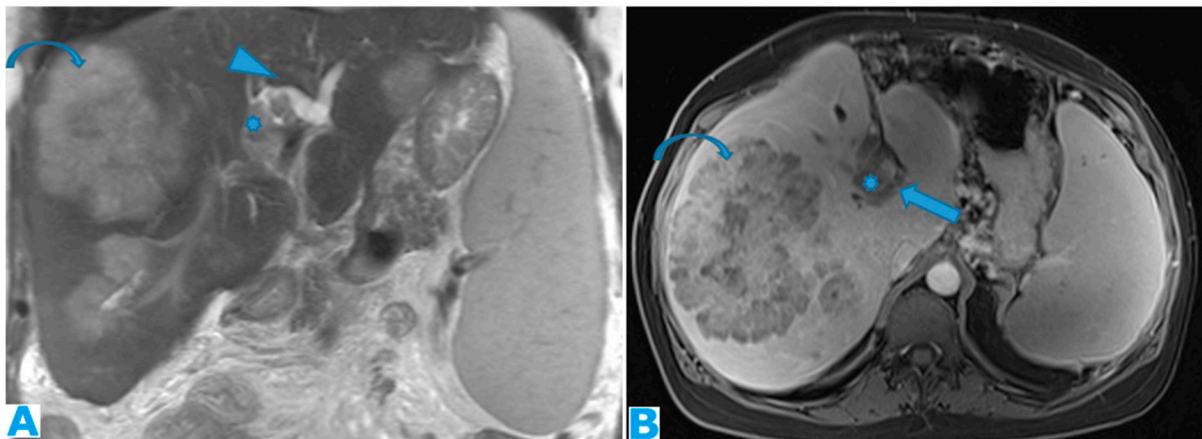

Figure 13. Coronal T2WI (**A**), axial CE portal phase FST1WI (**B**). PC from colon adenocarcinoma: periportal deposit (*) that causes segmental intrahepatic biliary dilatation (arrowhead) and portal vein compression (arrow). The patient had a known portal hypertension due to massive hepatic metastases (curved arrow) and splenomegaly.

3.1.4. Lesser Omentum

This portion of the peritoneum suspends the liver and the lesser curvature of the stomach and separates the first two centimetres of the duodenum from the liver. It is formed by the gastrohepatic and hepatoduodenal ligaments.

Deposits within this space show features common to any fat-containing space. Furthermore, since the porta hepatis runs in the hepatoduodenal ligament, biliary obstruction or portal vein compression may be found as indirect signs of PC (Figure 14).
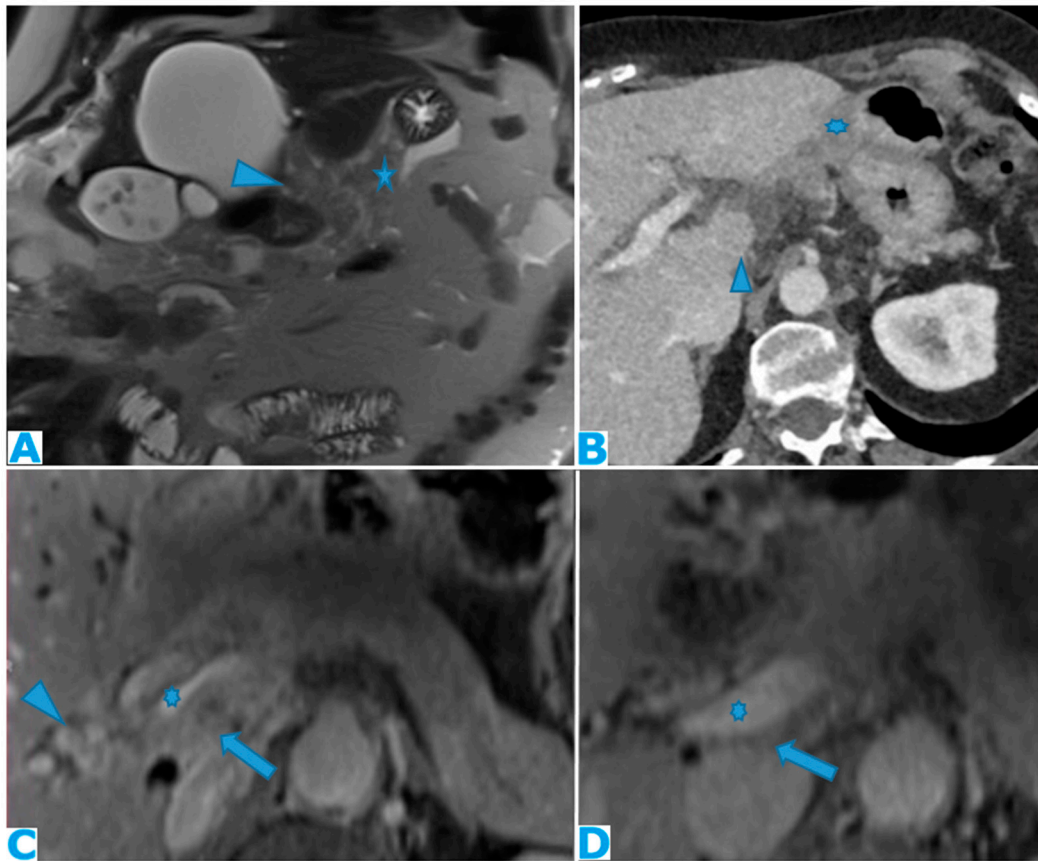
Figure 14. Axial CE-CT (**A**). PC from ovarian carcinoma: deposits within the gastrohepatic (*) and the hepatoduodenal ligaments (arrowheads). Coronal T2WI (**B**). PC from ovarian carcinoma: deposits within the lesser omentum: Identify its two components, the gastrohepatic (*) and the hepatoduodenal (arrowhead) ligaments. Axial CE portal phase FST1W1 (**C-D**), the current study (**C**) and from one year prior (**D**), for comparison. PC from colon adenocarcinoma: Deposits within the gastrohepatic ligament (lesser omentum) (arrows). Note the compression of the portal vein (*) on **C** and the development of collateral vessels (arrowheads).

As previously seen, once the disease is in the lesser omentum it can easily spread to the periportal space, thanks to the surrounding connective tissue of the Glisson sheath, which makes them continuous. This is a particularly important spread route for pancreatic and gastrointestinal tumours.

3.1.5. Lesser Sac

Potential space between the pancreas and the stomach. Its distention, either by a solid lesion or by ascites, as will be reviewed later, is a sign of its involvement by PC (Figure 15). It communicates with the rest of the peritoneal cavity (greater sac) through an opening, immediately posterior to the lesser omentum, the foramen of Winslow.
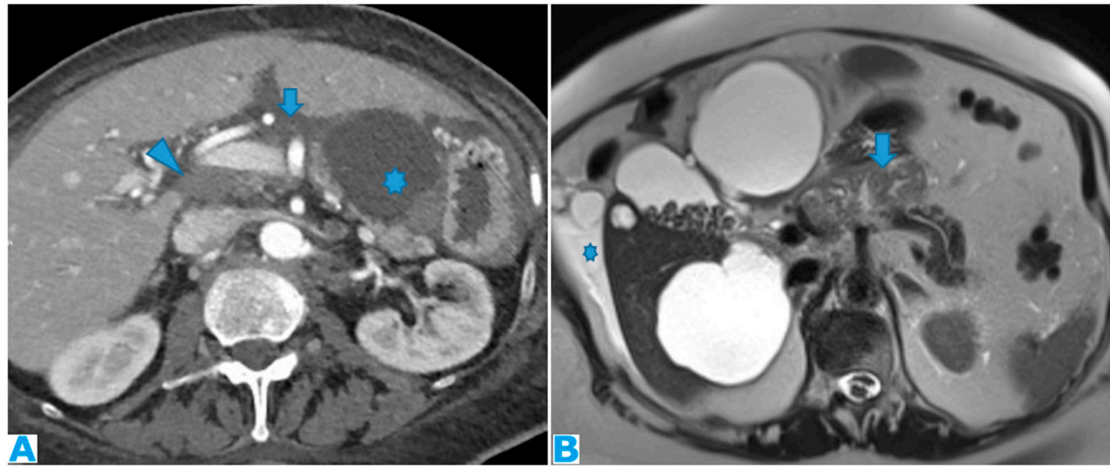
Figure 15. Axial CE-CT (**A**). PC from ovarian carcinoma: mass-like deposit within the lesser sac (*).
Also notice the seeding within the lesser omentum (arrow). Portacaval lymph node (arrowhead).
Axial T2WI (**B**). PC from ovarian carcinoma: mass-like deposit within the lesser sac (arrow). Ascites
(*).

3.1.6. Right Subhepatic Space

Pouch inferior to segment VI of the liver. It communicates with the right subphrenic space, the
right paracolic gutter and the lesser sac. Deposits within this space tend to be more subtle, partly due
to small size of this space, and range from an ill-defined outer hepatic contour to focal fat stranding
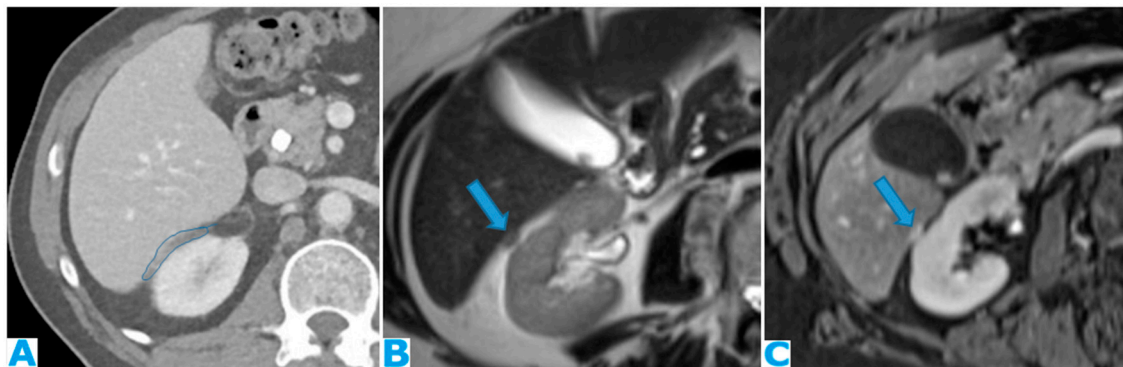and nodules (Figure 16).

Figure 16. Axial CE-CT (**A**): PC from breast carcinoma: deposits within the subhepatic space as
reticulation of its fatty content. Axial T2WI CE-CT (**B**), CE portal phase FST1WI (**C**): PC from colon
carcinoma: nodular deposit within the subhepatic space (arrow).

3.2. Inframesocolic Spaces

Inframesocolic spaces will also be described through the same cranial-to-caudal and lateral-to-
medial approach: greater omentum, paracolic gutters, small bowel mesentery, sigmoid mesocolon
and pelvis recesses.

3.2.1. Greater Omentum

The greater omentum is the main peritoneal fold. It connects the stomach to the anterior surface
of the transverse colon and then extends caudally into the pelvis covering the small bowel loops. It
lies mainly inferior to the transverse colon mesocolon though its smaller cranial portion (the
gastrocolic ligament) is within the supramesocolic space.

The uniqueness of the imaging features of deposits in this location is the omental cake, which occurs when nodular deposits collide (Figure 17) and blend through one another boosting a fibrotic response and replacing the omental fat (Figure 18).
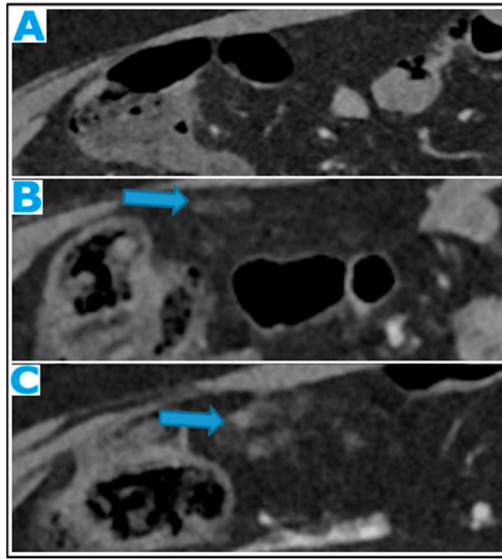

Figure 17. Axial CE-CT (**A**): from one year prior (disease-free peritoneum), **B** from four months prior, **C** current follow up. Note the early stages and evolution of omental deposits (arrows).
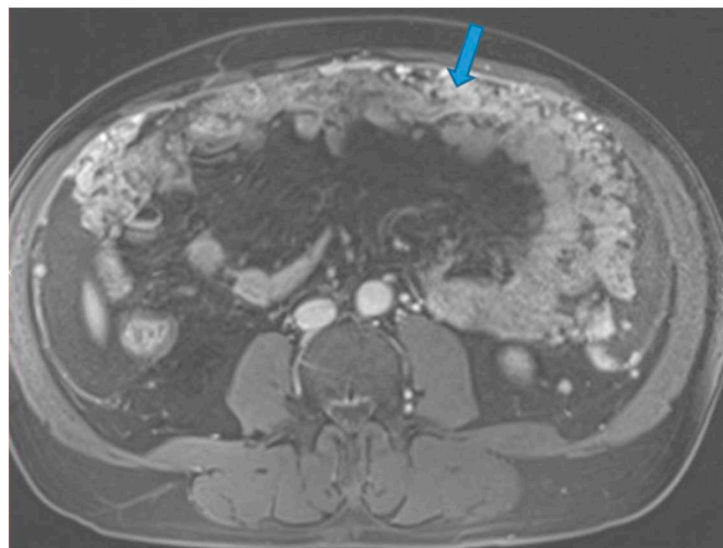

Figure 18. Axial CE portal phase FST1W. PC from melanoma: Omental cake (arrow) replacing the omental fat.

A helpful diagnostic sign, as the infiltration progresses, is the subsequent displacement of the bowel loops. Enlargement of the fatty content and mass effect due to omental seeding may be more apparent than the actual deposits (Figure 19).
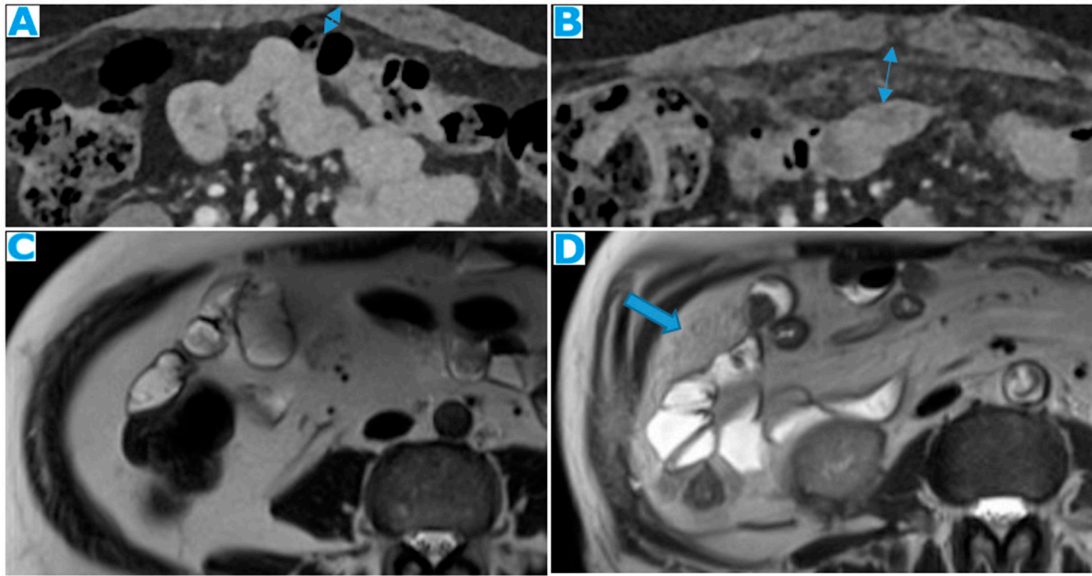
Figure 19. Axial CE-CT (**A** from one-year prior, **B** current follow up). PC from breast carcinoma: Note the omental infiltration on **B** associated with a posterior displacement of the small bowel loops. Axial T2WI (**C** peritoneal-disease-free study from two years prior, **D** current follow up). PC from renal cell carcinoma: Enlargement of the fatty content and mass effect due to omental seeding (arrow) that may be more conspicuous than the actual deposits.

Omental deposits are more easily detected on MR. However, in the early stages and especially in thin patients, CT appears to perform better, even though the scarce fatty content in thin patients may negatively contribute to identifying peritoneal deposits (Figure 20).
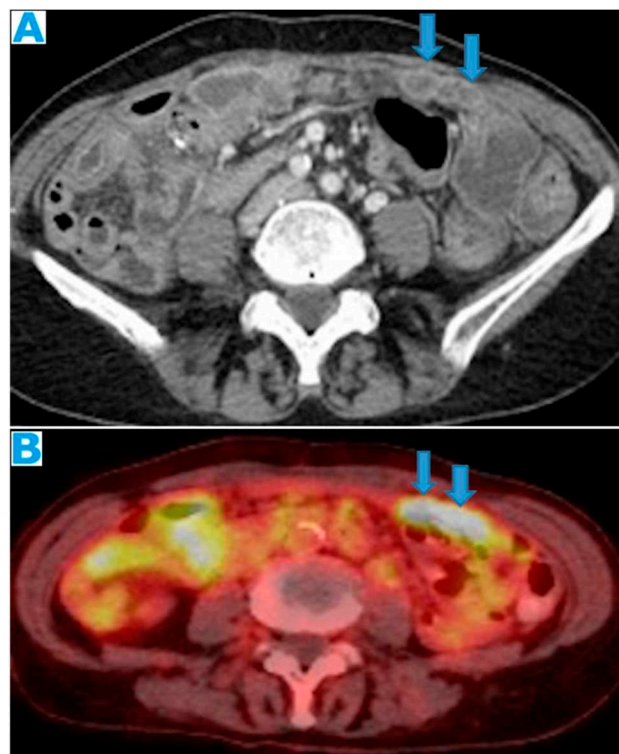

Figure 20. Axial CE CT (**A**), FDG PET CT (**B**). PC from colon adenocarcinoma: Nodular deposits within the omentum that were originally mistaken for SB loops on CT, due to scarce intrabdominal fat.

3.2.2. Small Bowel Mesentery

The small bowel mesentery is a fan-shaped peritoneal double layer that surrounds the small bowel and then extends diagonally from the ligament of Treitz in the left upper quadrant to the ileocecal junction, anchoring at these two locations and at the posterior parietal peritoneum.

Mesenteric deposits show a rather unique and more complex appearance when compared to deposits elsewhere in the abdominal cavity. Deposits may be found:

- <u>within the mesenteric fat</u>: As in the rest of the fat containing peritoneal spaces, they may range from focal nodular fat stranding to irregular haziness to nodules and masses (Figure 21).
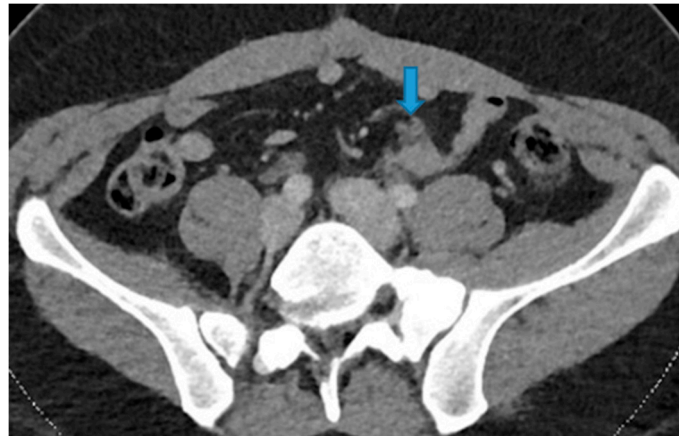

Figure 21. Axial CE-CT. PC from colon adenocarcinoma: Nodular deposit within the mesentery.

- <u>within the SB and caecal serosa</u>: Deposits may also lie within the serosa covering the small bowel and the caecum (Figure 22).
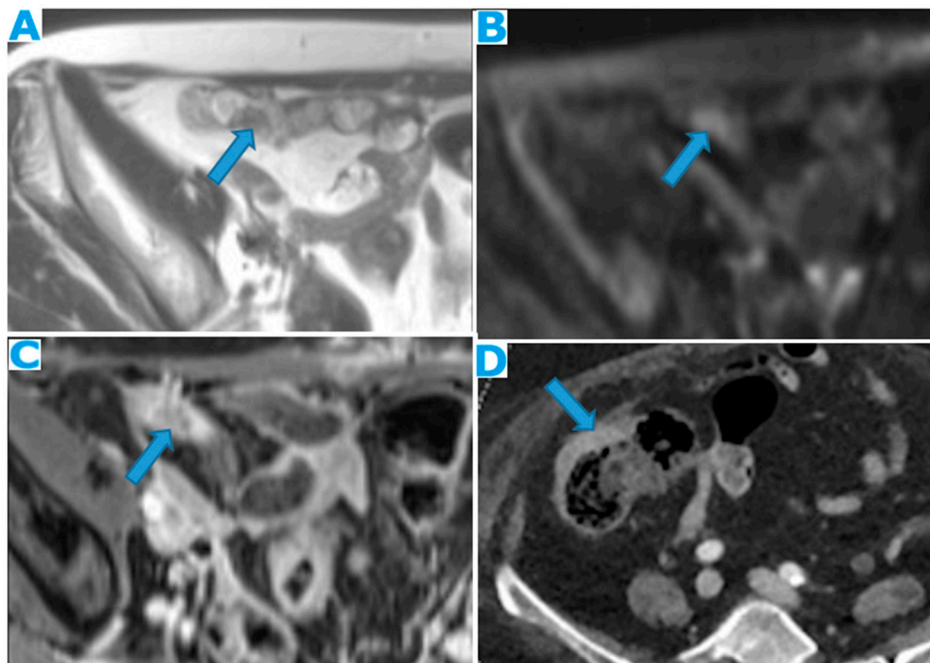

Figure 22. Axial T2WI (**A**), axial DWI (**B**), CE portal phase FST1WI (**C**). PC from duodenal adenocarcinoma: Deposit within the distal ileum serosa. Axial CE-CT (**D**). PC from breast carcinoma: Deposits within the caecal serosa.

- <u>involving both the mesentery and the serosa</u>: As in the transverse mesocolon, deposits may appear both within the mesentery and the serosa covering the small bowel loops and the caecum (Figure23).
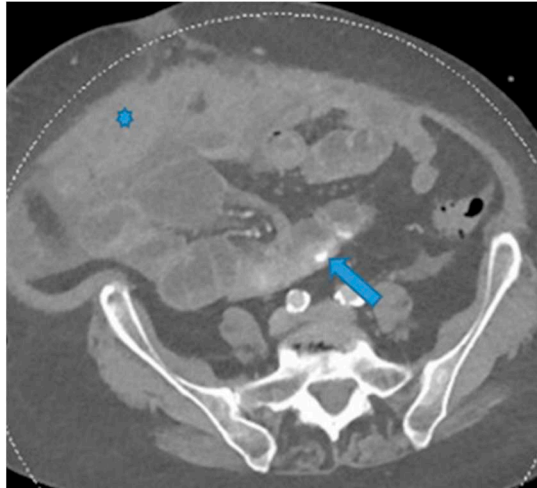
Figure 23. Axial CE-CT. PC from ovarian carcinoma: mesenteric seeding. Mesenteric involvement may happen as a combination of deposits involving both the mesentery and the bowel serosa, as in this case. Observe the clustered SB loops appearance. The calcified content of some of the deposits enhances their presence (arrow). Omental deposits (*).

- within the mesenteric leaves: Deposits within the mesenteric leaves may go unperceived. The nodular thickening and enhancement of the mesenteric leaves is usually more conspicuous on MR but can be also spotted on CT and it becomes more noticeable when accompanied by ascites (Figures 24 and 25).
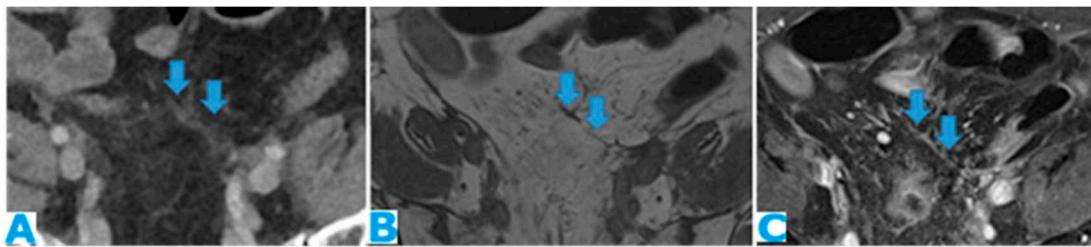

Figure 24. Axial CE-CT (**A**), axial T2WI (**B**), axial CE portal phase FS T1WI (**C**). PC from endometrial carcinoma: Deposit seeding within the mesenteric leaves.
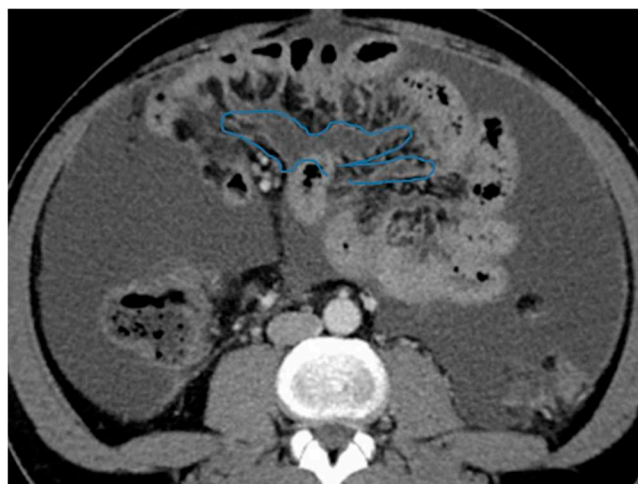

Figure 25. Axial CE-CT. PC from colon adenocarcinoma: Involvement of the mesenteric leaves (note the nodular thickening and enhancement) that becomes more apparent with ascites.

- Stellate mesentery: Diffuse mesenteric infiltration leads to a stellate appearance, which is commonly associated with breast (especially lobular carcinoma) [16], gastric, pancreatic, and ovarian tumours [17]. This deposition pattern follows the distribution of the mesenteric vessels, causing thickening and rigidity of perivascular bundles (Figure 26).
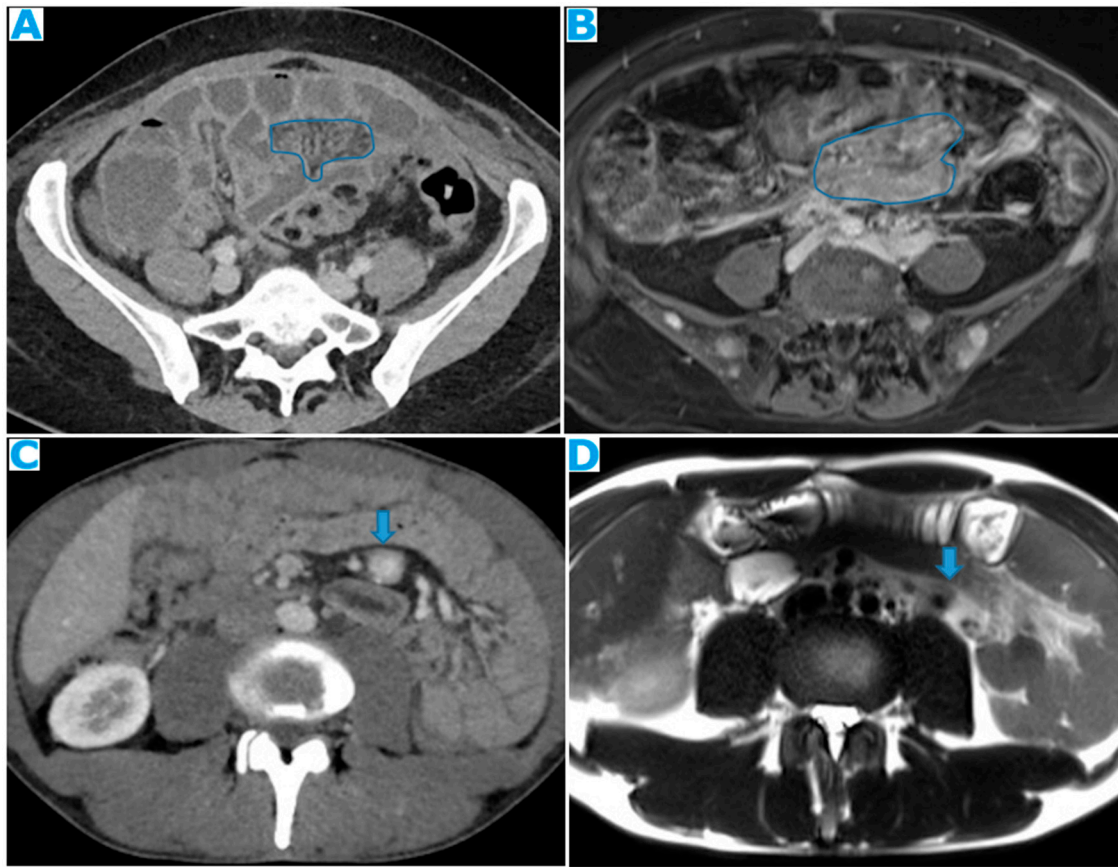

Figure 26. Axial CE-CT (**A**). PC from stomach adenocarcinoma: Stellate mesentery. Axial CE portal phase FST1WI (**B**). PC from lobular breast adenocarcinoma: Stellate mesentery, notice the perivascular distribution. Axial CE-CT (**C**), axial T2WI (**D**). PC from stomach adenocarcinoma: Isolated perivascular deposit within the mesentery, as a soft tissue mass surrounding a branch of the SMV.

As a result of tumour infiltration, the mesentery becomes rigid and loses its usual free wavering. SB loops will appear thickened, with restricted distensibility, looking initially separated and angulated and finally, clustered (Figure 27). With time, the retraction caused by the deposits will cause a decrease in size of the mesenteric fat (Figure 28). These effects on the SB loops and the mesenteric fat may happen to be more conspicuous than actual deposits.
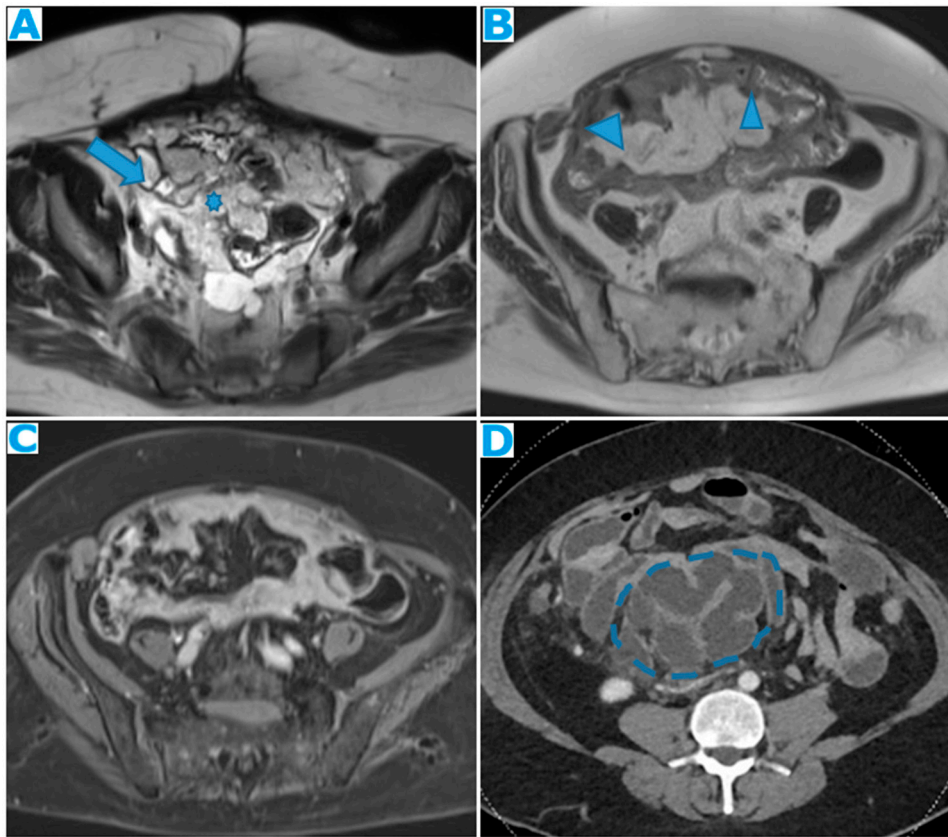
Figure 27. Axial T2WI (**A**). PC from mucinous adenocarcinoma of the uracus: Notice the hyperintense mesenteric deposits (*) (signal due to mucin content) and how the SB loops appear separated and angulated (arrow). Axial T2WI (**B**), axial CE portal phase FST1WI (**C**). PC from breast carcinoma: Mesenteric deposits (arrowheads on B) make SB loops appear thickened and separated. Notice how deposits are more conspicuous on T2WI due to its high tissue contrast. Axial CE-CT (**D**). PC from ovarian carcinoma: Clustered small bowel loops as the end point of mesenteric seeding.
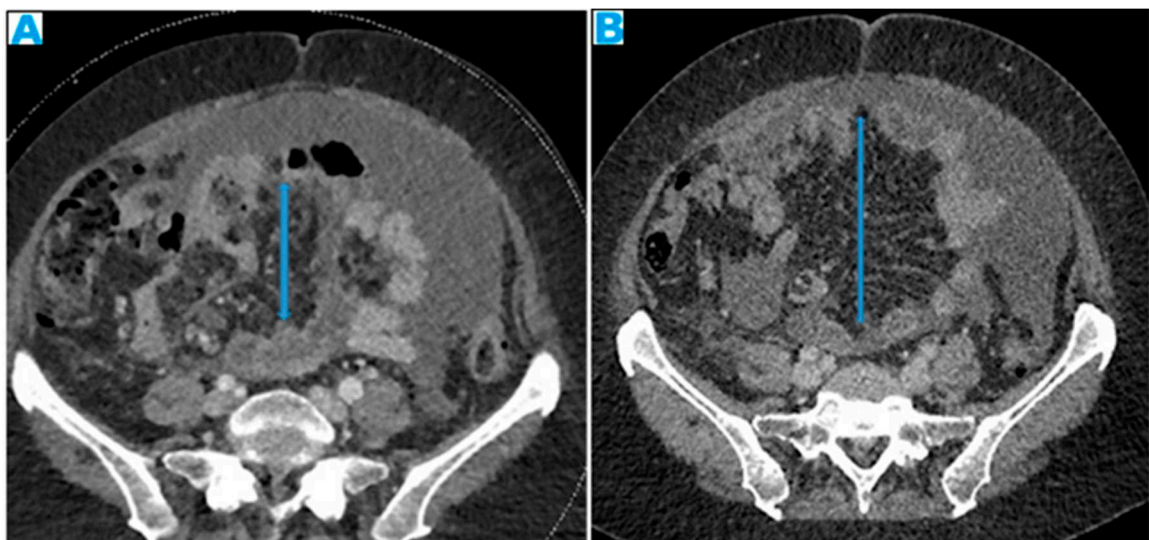

Figure 28. Axial CE-CT, current study (**A**) and from six months prior (**B**). PC from colon carcinoma: The mesentery becomes fibrotic as the seeding evolves and, secondary to the retraction effect, a decrease in size of the mesenteric fat will occur (arrows). This effect may be more conspicuous than the actual deposits.

The main complication of deposits lying within this space is bowel obstruction, which usually occurs at a late stage and its diagnosis is not challenging. However, it may also be the presenting sign. It typically involves more than one small bowel loop, and the degree of occlusion may vary. Another not so frequent complication is bowel ischaemia due to perivascular infiltration (Figure 29).
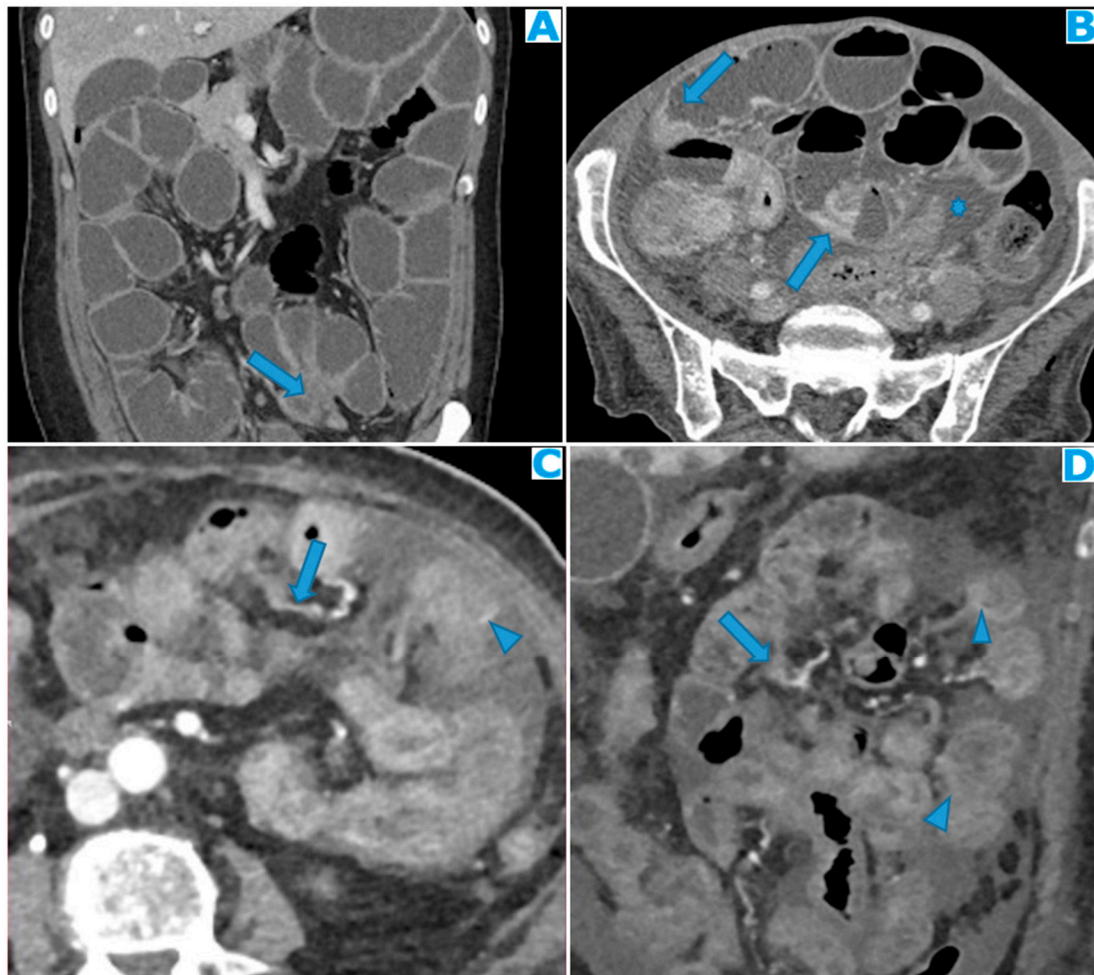

Figure 29. Coronal MPR (**A**). PC from mucinous colon adenocarcinoma: Solitary mesenteric deposit (arrow) as the cause of a SB obstruction, involving several loops. Axial CE-CT (**B**). PC from breast carcinoma: SB multifocal obstruction, due to several deposits within the SB serosa (arrows). Ascites (*****). Axial CE-CT (**C**) and coronal MPR (**D**). PC from adenocarcinoma of the urachus: Severe mesenteric infiltration causing SB ischaemia as distal SMA and SMV branches are compressed and infiltrated by deposits (arrows). Observe the SB loops thickening and the heterogenous and patchy bowel wall enhancement (arrowheads) due to the ischaemia.

3.2.3. Paracolic Gutters

Peritoneal recesses between the colon, partially covered by the posterior parietal peritoneum (on its anterior, medial, and lateral walls) and the lateral parietal peritoneum on each side. They constitute the attachments of the ascending and descending colon to the posterior parietal peritoneum.

Both are in continuity with the peritoneal spaces in the pelvis. Superiorly, the right paracolic gutter communicates with the right subphrenic and right subhepatic spaces, whereas the left paracolic gutter, much smaller, is partially separated from the left subphrenic space, by the phrenicocolic ligament (Figure 1b).

The infiltrated peritoneum will typically appear nodulary thickened showing pathological enhancement (Figure 30).
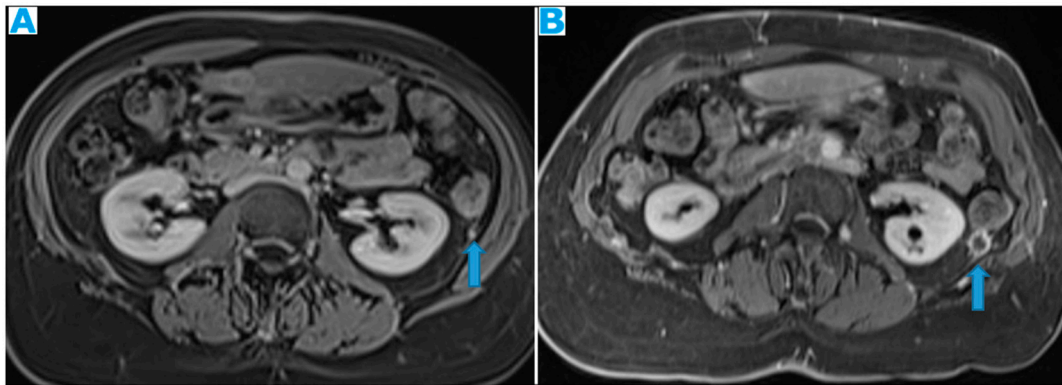

Figure 30. CE portal phase FST1WI (**A**, from four months prior, **B**, current study). PC from colon adenocarcinoma: Nodular deposit within the left paracolic gutter that was undercalled. See the growth on **B**.

The oblique orientation of the small bowel mesentery described earlier divides the inframesocolic compartment into two compartments: right and left, the latter being larger. The only structure standing on the way of the free communication between the left inframesocolic space and the pelvis is the sigmoid mesocolon, thus the reason why it constitutes a common site of deposits, as it is an area of arrested flow.   Deposits within the sigmoid mesocolon will lie on its fat and/or on the serosa and differentiation between them may not always be feasible. Sigmoid luminal stenosis with/without signs of obstruction are a frequent consequence of the seeding (Figure 31).
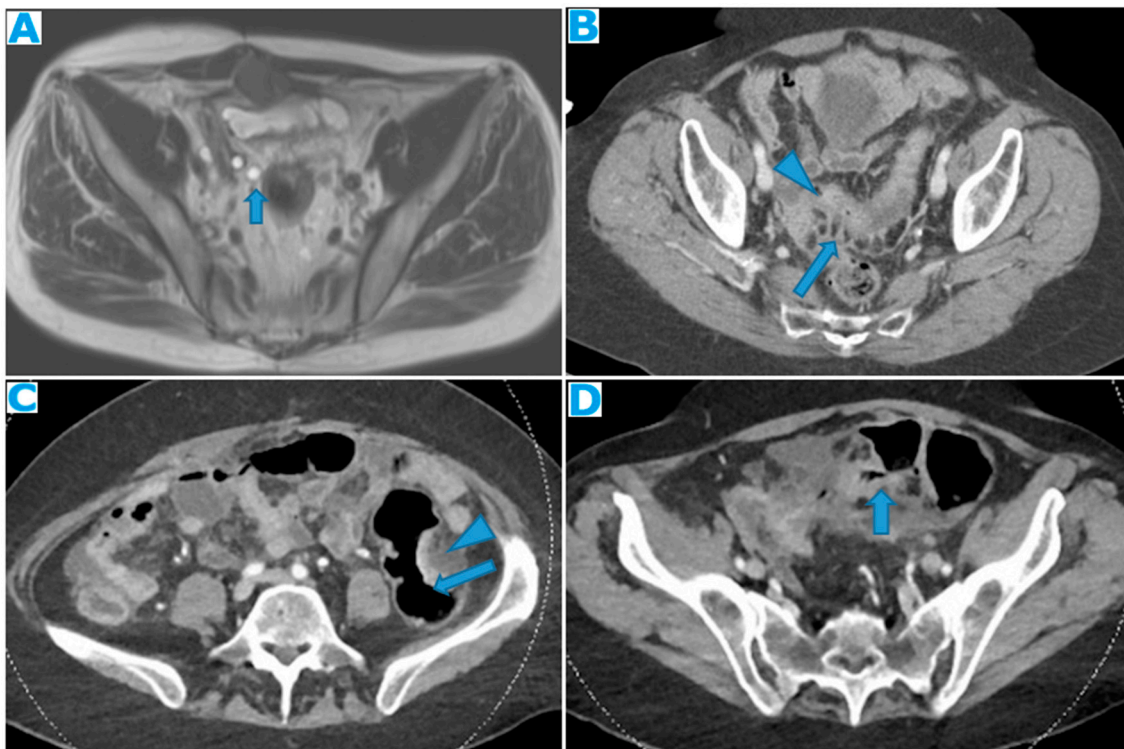
Figure 31. Axial T2WI (**A**). PC from mucinous adenocarcinoma of the terminal ileum: Hyperintense nodular deposits (due to mucin-content) within the sigmoid mesocolon. Axial CE-CT (**B**). PC from undifferentiated carcinoma of unknown origin: Deposits within both the sigmoid mesocolon (arrows), outlining the epiploic appendices, and within the sigmoid serosa, making the sigmoid colon appear thickened (arrowheads). Axial CE-CT (**C**, **D**). PC from colon adenocarcinoma: **A**. Observe on **C** the seeding involving the sigmoid mesocolon (arrowhead) and the serous layer of the bowel

(arrow), partially obstructing the sigmoid lumen. On **B** the two components cannot be differentiated but a luminal stenosis is clearly identified (arrow).

The mesentery of the appendix is anchored to the lower end of the small bowel mesentery, close to the ileocecal junction and to the tip of the appendix. Despite its small size, it may be an important site in appendiceal neoplasms: in case of rupture, deposits will likely appear there first.

3.2.4. Peritoneal Recesses of the Pelvis-Ovarian Metastases

Deposits within the pelvis may be quite tricky to find as the anatomy is rather complex and there are several structures that fit in a small cavity, therefore a careful exploration using multiplanar reconstructions is recommended.

The parietal peritoneum that covers the abdominal wall goes down to the pelvis, where it does not reach the pelvis floor, as it reflects on the pelvis organs (peritoneal reflexion). The peritoneal reflexion covers the dome of the urinary bladder, then descends along its posterior wall and laterally forms the paravesical spaces: a fold over the ureters, and in men, it also covers the deferent ducts and the seminal vesicles.   It continues towards the rectum and then ascends partially cloaking the upper and middle rectum (thus subperitoneal, the rest is extraperitoneal) and the lateral pelvic walls (Figure 32).   In women, it also coats the uterine fundus and body and the posterior part of the vagina and extends laterally (broad ligament) wrapping up the tubes and suspending the ovaries.
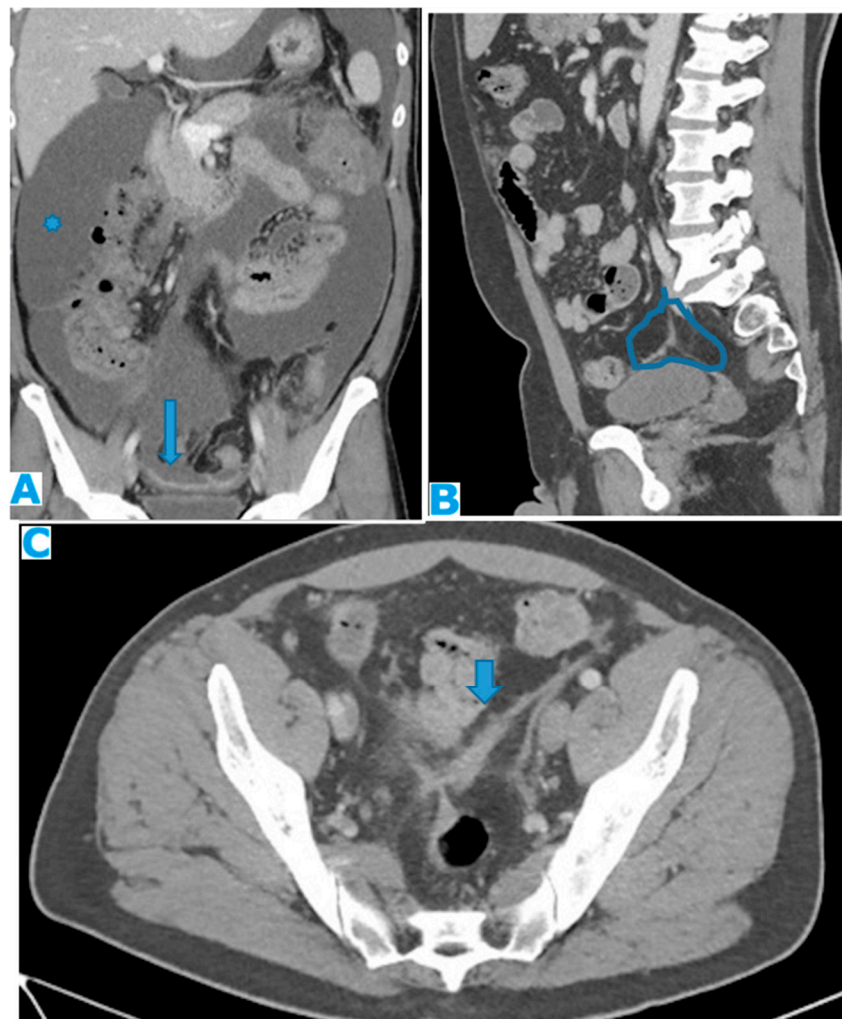

Figure 32. CE-CT Coronal MPR (**A**). PC from colon carcinoma: Observe how the parietal peritoneum does not reach the pelvis floor. Ascites (*). Deposits within the pelvic reflexion (arrow). Sagittal MPR (**B**), axial CE-CT (**C**). PC from adenocarcinoma of the appendix: Irregularly thickened peritoneal

reflexion due to seeding. Observe on the sagittal MPR how the peritoneal reflexion covers the dome of the urinary bladder and then descends, following its posterior wall.

Two blind-ends pouches are therefore found in women: the uterovesical, anteriorly and the rectouterine, posteriorly, while there is only one in men, the rectovesical [4].

Pelvic organs, except for the tubes, which are intraperitoneal, are only covered by the peritoneum superiorly and laterally. Thus, deposits will be identified as enhancing nodular peritoneal thickenings, either on the pelvic walls (Figure 33) or within the peritoneal reflexion, either surrounded by fat or on the partially peritonealised organ surfaces (Figure 34).
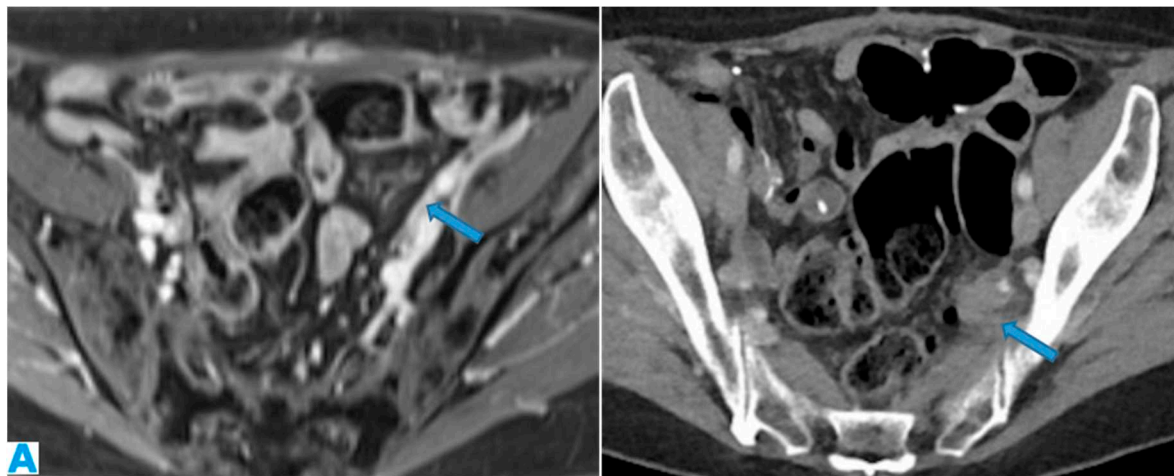

Figure 33. Axial CE portal phase FST1WI (**A**). PC from duodenal adenocarcinoma: Deposit seeding within the peritoneum that covers the left pelvic wall, which looks diffusely thickened (arrow). Axial CE-CT (**B**). PC from undifferentiated caecal adenocarcinoma: Nodular deposit within the peritoneum that covers the left pelvic wall (arrow).
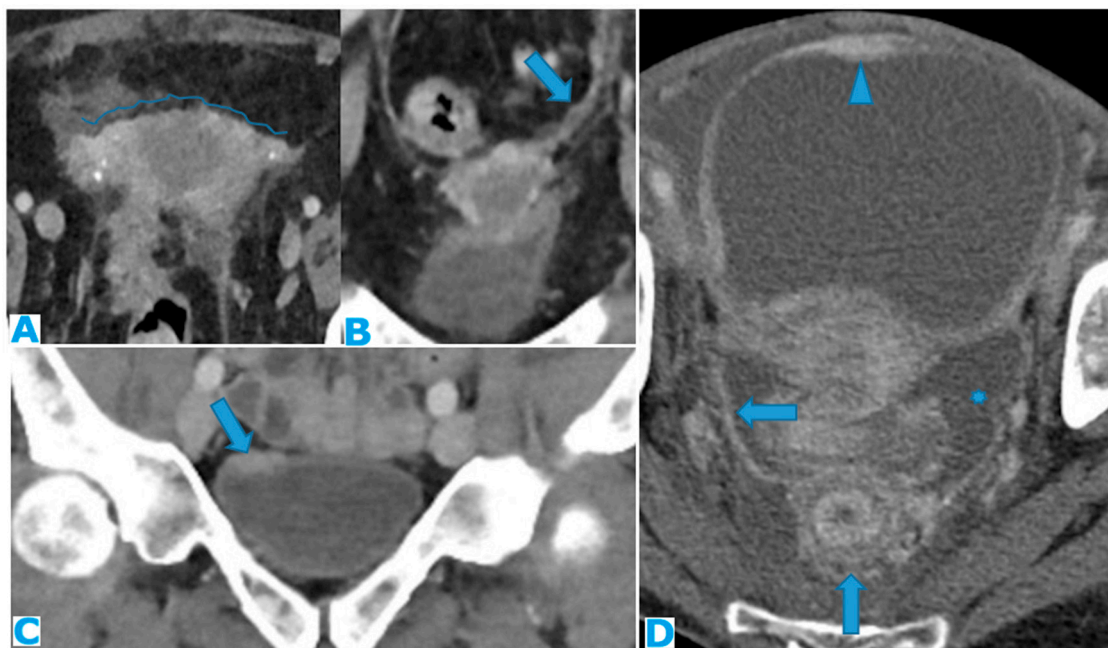
Figure 34. Axial CE-CT (**A**), CE-CT coronal MPR (**B**). PC from breast carcinoma: The peritoneal reflexion covers the uterine fundus and body and the posterior part of the vagina and extends laterally (broad ligament, arrow on **B**). Note the nodular appearance of the peritonealised uterine surface and the broad ligaments (arrow on B) due to deposit seeding. CE-CT coronal MPR (**C**). PC from cardia adenocarcinoma: Deposit within the peritoneal reflexion covering the vesical dome (arrow). Axial CE-

CT (**D**). PC from breast carcinoma: Notice the peritoneal seeding on the peritonealised surfaces of the bladder (arrowhead), and rectum (vertical arrow). Also, within the peritoneum that covers the pelvic walls (horizontal arrow). Ascites (*).

As ureters are in close contact with the peritoneum at the paravesical spaces, pelvis deposits may be the cause of ureterohydronephrosis and this is frequently overlooked, especially as the only sign of PC. Any deposit along the posterior parietal peritoneum in the proximity of the course of the ureter may also be the cause of a urinary obstruction, but the pelvis is a very frequent location (Figure 35).
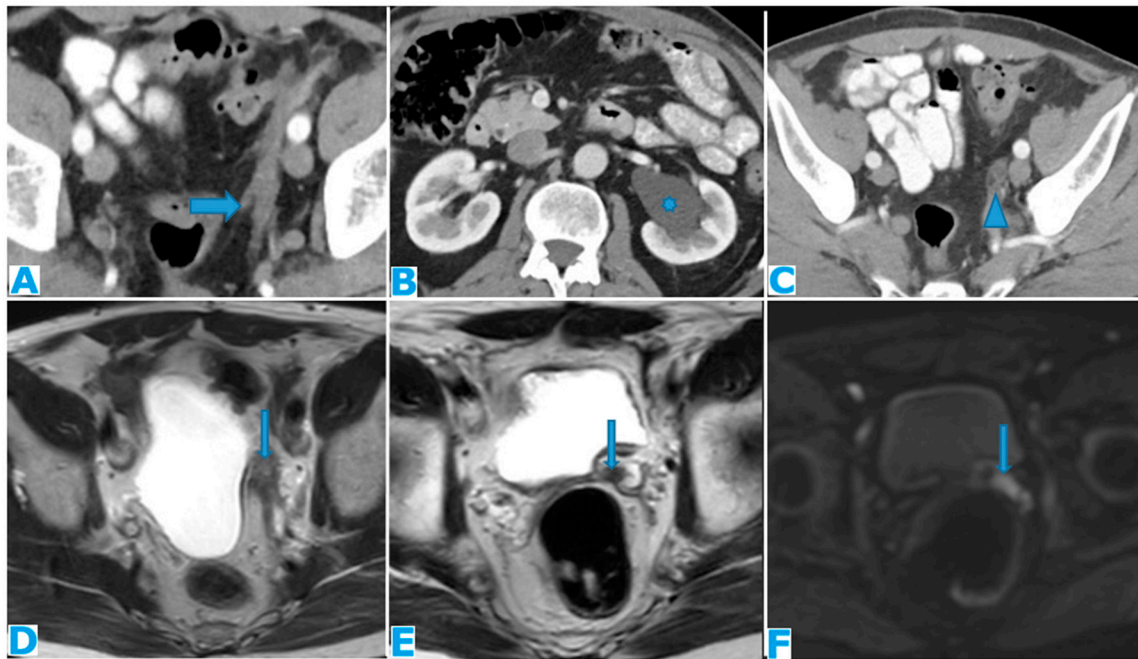

Figure 35. Axial CE-CT (**A**, **B**, **C**). Axial T2WI (**D** and **E**), DWI (**F**). PC from mucinous adenocarcinoma of the appendix: Notice the peritoneal deposit within the left lateral pelvis (arrow on **A**) as an elongated soft tissue mass. The patient presented with a left uretero-hydronephrosis (* on **B**) due to the pelvic deposit which obstructed the ureter (arrowhead on **C**). Paravesical spaces are peritoneal recesses that cover on each side the distal ureter, the seminal vesicle, and the deferent duct. Note the deposit within the left paravesical space and how it obstructs the left ureter (arrow on **C**). The deposit also follows the course of the left deferent duct (arrow on **E** and **F**).

As a result of pelvis deposits within the peritonealised portion of the rectum, occlusion may occur.

Another common site of PC in the pelvis is the ovaries. As seen previously, they are extraperitoneal organs but considered intraperitoneal as they communicate with the peritoneal cavity. This is the reason why ovaries are included amongst the locations of PC.

Compared to primary ovarian tumours, ovarian metastases seem to be smaller, more frequently bilateral, showing more uniform cysts and more moderate enhancement of the solid portions [18]. Although a solid appearance may also be found or even characteristics resembling the primary tumour (Figure 36).
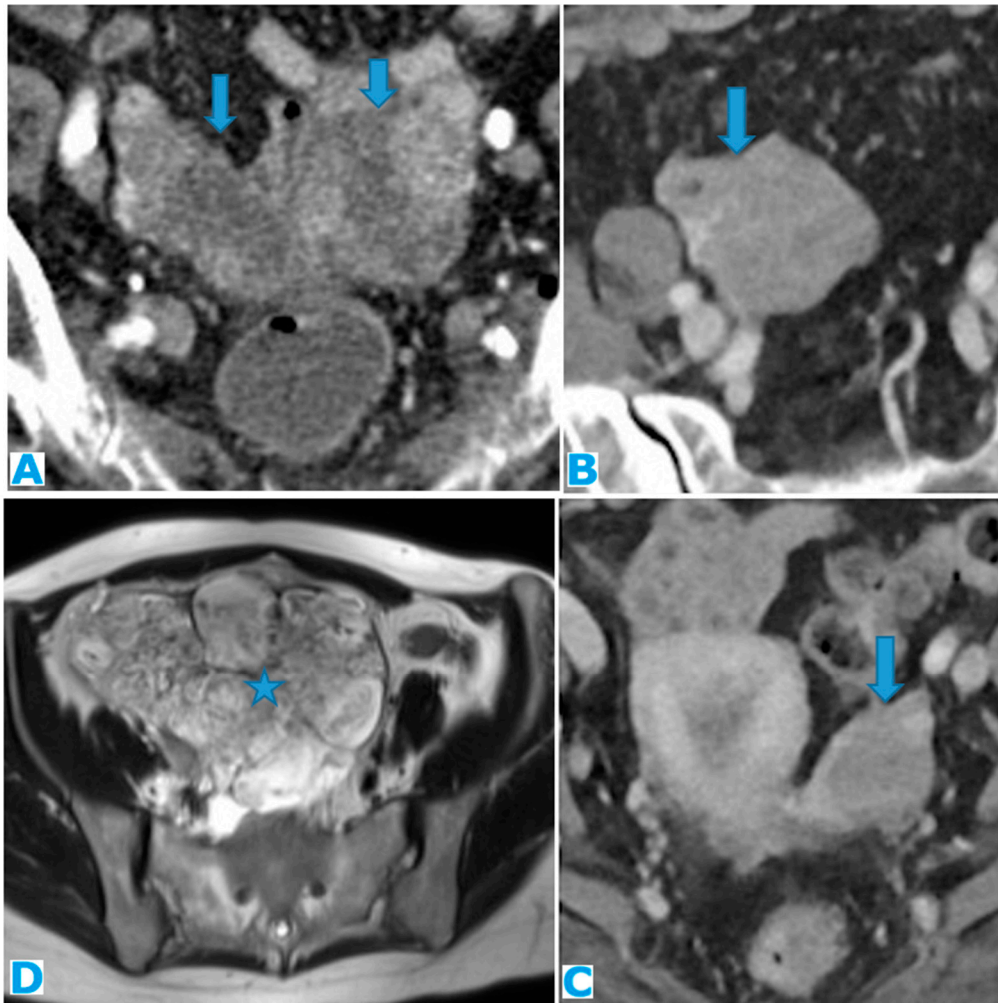
Figure 36. Axial CE-CT (**A**). PC from sigmoid adenocarcinoma: Bilateral ovarian metastasis as complex cystic masses with solid poles. Axial CE-CT (**B**, **D**). PC from colon adenocarcinoma: Bilateral ovarian metastasis as solid masses. Axial T2WI (**C**). PC from mucinous tumour of the appendix: Left ovarian metastases (*) presenting as a predominantly hyperintense mass due to the mucin content.

The term Krukenberg tumour is sometimes misused in the setting of ovarian metastases from a gastrointestinal tumour, as its use should be limited to ovarian metastasis from a poorly differentiated adenocarcinoma with signet ring cell features [19]. Krukenberg tumour should be considered in the differential diagnosis when solid bilateral ovarian masses containing intratumoral cystic component are detected, even in the absence of a primary malignancy [20].

4. Peritoneal Fluid Circulation-Ascites

Now that the peritoneal anatomy has been revised, the focus will be placed on the fluid contained in the peritoneal cavity, as it will play a determinant role in the seeding of the deposits.

Peritoneal fluid circulates following the path determined by ligaments and mesenteries, under the influence of the abdominal pressure fluctuations caused by respiration and intestinal peristalsis.

In case of tumour spread to the peritoneum, the quantity of peritoneal liquid will rise due to two conditions: the obstruction of the lymphatics in charge of the resorption and the over-production of fluid caused by the vascular permeability factor secreted by the tumour cells [21,22].

Fluid in the inframesocolic space naturally goes down on the right of the small bowel mesentery [23], through the mesenteric leaves, and on the left, through the medial mesosigmoid, thus an area of arrested flow. It then reaches the pelvic recesses, the most gravity dependent spaces. After filling the pelvis, it goes up the paracolic gutters: preferently on the right, as the left gutter is shallower, and

the flow is limited cranially by the phrenicocolic ligament [24] (Figure 1b). On the right, it reaches the subhepatic space and finally, the right subphrenic space, where most of the peritoneal lymphatic clearance will take place, along with the omentum [25]. Therefore, places that normally constitute a free route or barrier for the flow or where most of the resorption takes place, need to be particularly scrutinized.

Table 1 sums up the favoured locations for the peritoneal seeding and the underlying reasons.

Table 1. Favoured PC sites and underlying reasons.

Favoured PC sites	Underlying Reason
Ileocecal region	Anchor of the small bowel mesentery
Sigmoid mesocolon	Area of arrested flow
Right paracolic gutter	Major gravity dependent pathway
Subhepatic space	Gravity dependence
Right subphrenic space and omentum	Resorption sites

Ascites may be one of the first signs of PC. Its appearance correlates closely with its volume: if minimal will only be found in the pelvic recesses, surrounding the liver and the spleen or between the small bowel loops, in a triangle-shaped fashion (Figure 37). If quantity increases, it will fill up the gutters, the omentum, and the mesentery leaves.
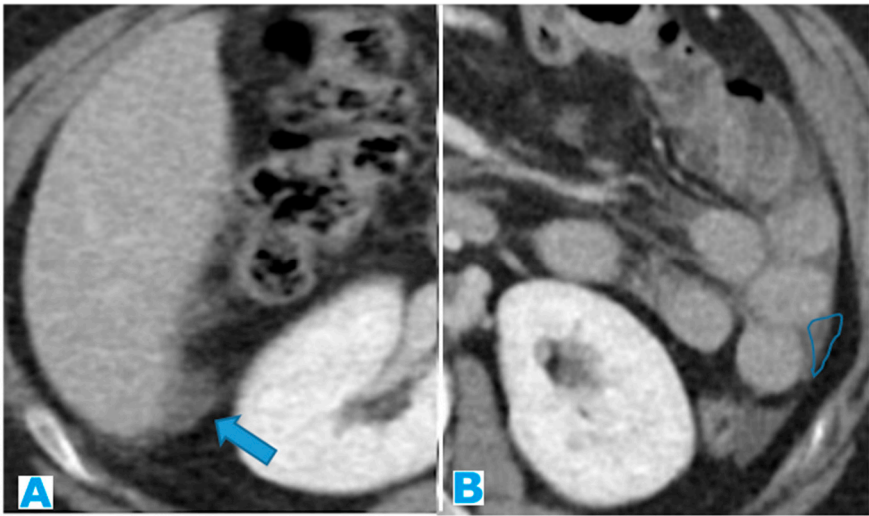

Figure 37. Axial CE-CT (**A**, **B**). PC from ovarian carcinoma: Minimal ascites within the subhepatic space (arrow on **A**) and between the SB loops, triangle shaped (**B**).

Suspicious signs may be ascites with rounded or bulging contours or when present concomitantly in the greater and lesser sacs (Figure 38).
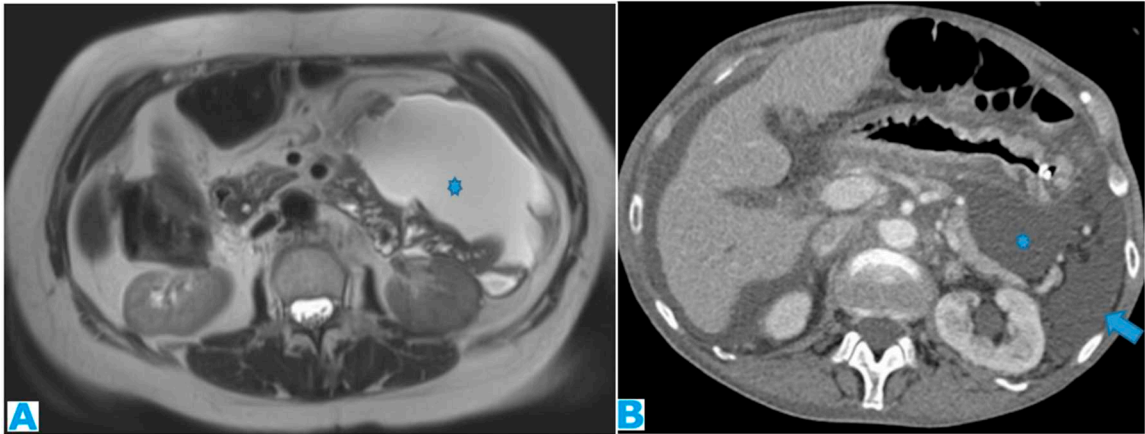
Figure 38. Axial T2WI (**A**). PC from ovarian adenocarcinoma : Loculated ascites within the mesentery (*). Axial CE-CT (**B**). PC from breast carcinoma: Concomitant ascites within greater (arrow) and lesser (*) sacs.

Another important clue is how SB loops behave to peritoneal liquid: in non-neoplastic ascites or in early stages of PC, they will float freely, with an anterior location, whereas in advanced PC, as the mesentery becomes fibrotic and rigid, SB loops will be pulled back centrally and posteriorly (the tethered-bowel sign) {26}. Characteristically, there will be little quantity of fluid between these rigid infiltrated mesenteric leaves, while predominant elsewhere in the peritoneal cavity (Figure 39).
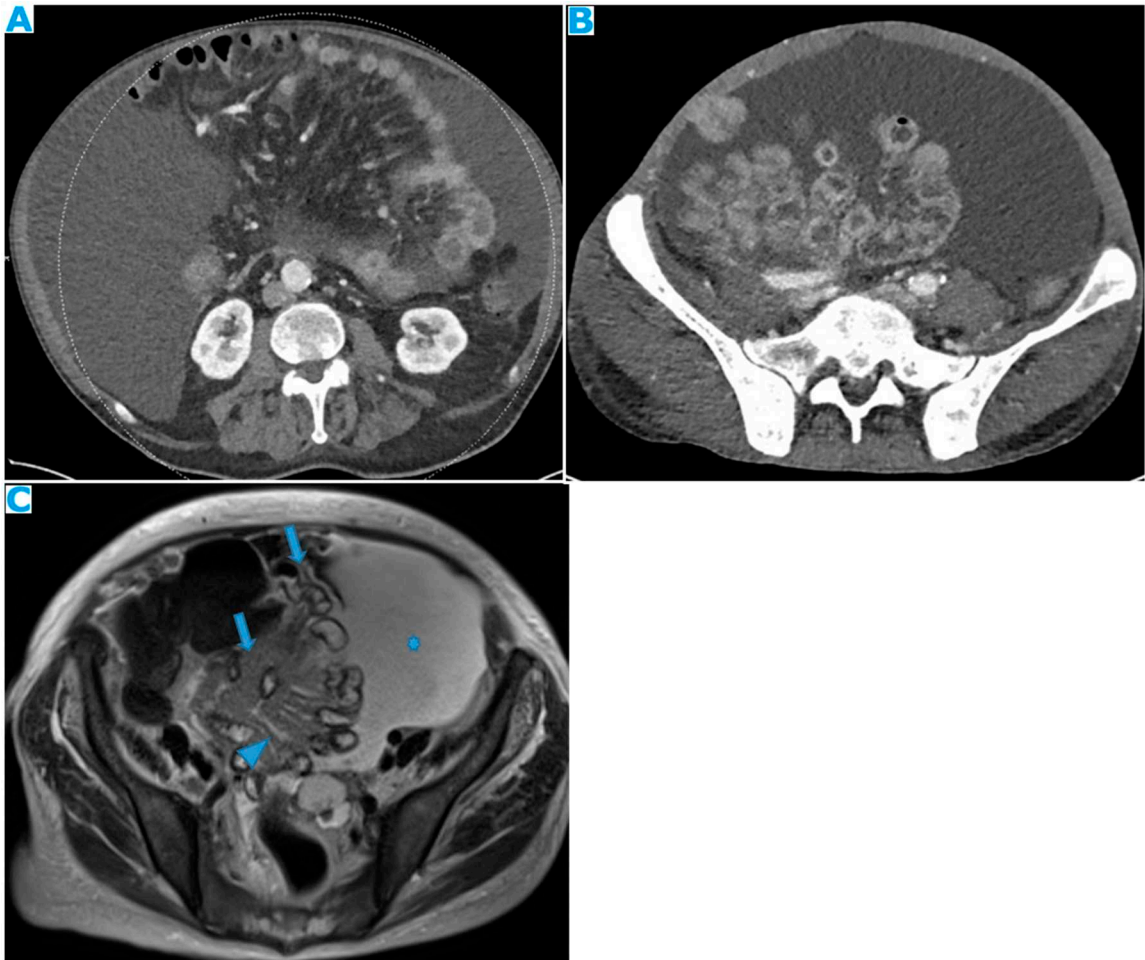
Figure 39. Axial CE-CT (**A, B**). **A** : non-malignant ascites, **B** : malignant ascites from colon adenocarcinoma. Observe how SB loops float freely on **A**, with an anterior disposition. On a malignant ascites (**B**), SB loops are drawn posteriorly and lose contact with the anterior abdominal wall (tethered-bowel sign) due to the rigid infiltrated mesenteric leaves. Axial T2WI (**C**). PC from endometrial carcinoma: Diffuse mesenteric deposit seeding (arrow) which causes SB retraction (tethered-bowel sign). Notice that despite massive ascites (*), there is scarce quantity of liquid between the rigid infiltrated mesenteric leaves (arrowhead).

In the setting of portal hypertension and non-malignant ascites, though, collateral vessels within the parietal peritoneum should be born in mind cautiously so as not to misdiagnose them as deposits (Figure 40).

Figure 40. Axial CE-CT. Observe the enhancing pseudonodular parietal peritoneum (arrows) which corresponds to collaterals vessels, not to be mistaken for peritoneal deposits.

5. Deposit Behaviour on Cross Sectional Images

Signal wise, the deposit does not fall far from the primary tumour, that is, deposits will usually show a density/signal intensity and enhancement pattern resembling the primary tumour, as extra-peritoneal metastases do.

Thus, one should always bear in mind the underlying histology and imaging features of the primary tumour and contemplate the possibility of a second primary tumour if a discrepancy is found.

In addition, in the event of no known primary tumour, which happens in about 3 to 5% of cases of PC [2], the behaviour on the different MR sequences and, on a lesser degree, on CT, may be helpful hints to suggest the origin, despite the non-specificity of the imaging findings.

Indeed, knowledge of the underlying deposit content responsible for the appearance of high signal intensity on T1 and T2 weighted images of peritoneal deposits is an important diagnostic criterion that can contribute to the diagnosis of the primary tumour.

Table 2 summarizes the behaviour of the peritoneal deposits according to their appearance on MR and CT, their content, and the corresponding primary tumour regardless of the cell line.

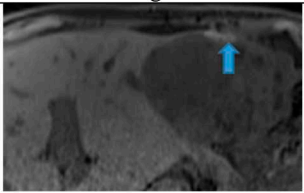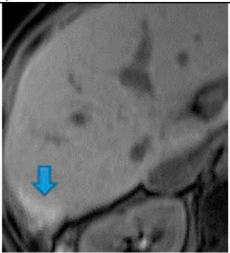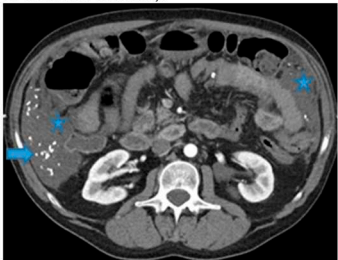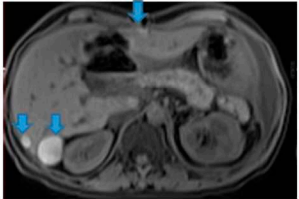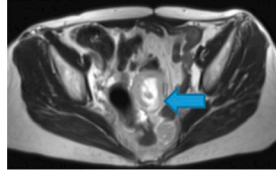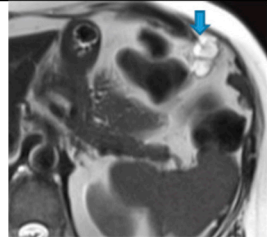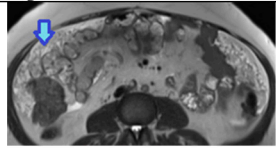| Content	T1	T2	CT	Primary tumour	Figures
Table 2. Behaviour of peritoneal deposits according to their appearance on MR and CT, their content and the corresponding primary tumour, regardless of the cell line.					
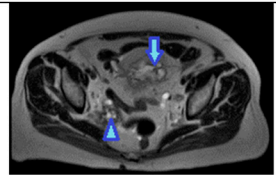
Content	T1	T2	CT	Primary tumour	Figures
Melanin	↑	↓	↓	Melanoma	Figure 41. Axial NE FST1WI. PC from melanoma: Note the hyperintense melanin-containing perihepatic deposits (arrow).
Calcium	↑=	↓=	↑	Mucinous tumors (ovary, stomach, colon, pancreas, appendix, gallbladder, urachus) Serous papillary ovarian tumour	Figure 42. Axial NE FST1WI.PC from serous ovarian adenocarcinoma: Hyperintense perihepatic deposits (due to calcified content). Figure 48. Axial CE CT. PC from colloid adenocarcinoma of the caecum: Observe the specks of calcification (arrows) scattered throughout the deposits (*).
Blood (*)	↑ ↑	↓ ↑	↑	Hypervascular tumours. High-grade ovarian tumours (serous and endometrioid adenocarcinoma). Clear cell ovarian carcinoma Granulosa cell tumour. (*) In the subacute stage of a haematoma, the methemoglobin causes a high SI on T1WI, and a variable SI on T2WI (low in early subacute stage, high in late subacute stage).	Figure 43. Axial NE FST1WI PC from serous ovarian adenocarcinoma: Blood-containing peri and subhepatic deposits (arrows).

Table 2. Behaviour of peritoneal deposits…… (continuation)					
Content	**T1**	**T2**	**CT**	**Primary tumour**	**Figures**
Myxoid	↓	↑	↓	Myxoid tumours	**Figure 44**. Axial T2WI. Myxoid leiomyosarcoma of the uterus: patient with pelvic deposits in the setting of a relapse. Observe the deposit central high SI on T2WI due to the myxoid content.
Non mineralized cartilage	↓	↑	↓	Condrosarcoma	**Figure 45**. Axial T2WI. Peritoneal deposit from rib condrosarcoma: Omental deposit showing high SI on T2WI, due to the non-mineralized cartilage content.
Mucin	↓	↑	↓	Mucinous tumours (ovary, stomach, colon, pancreas, appendix, gallbladder, urachus)	**Figure 46**. Axial T2WI. PC from mucinous adenocarcinoma of the urachus: Hyperintense omental-cake due to mucinous content.
Keratin	↓	↑	↓	Squamous differentiation	**Figure 47**. Axial T2WI. Bladder adenocarcinoma with a squamous differentiation. Observe the locally advanced vesical tumor (arrow). Note the right pelvic peritoneal deposit (arrowhead), showing the same imaging features as the tumour. The high signal on T2WI may be due to the keratin formed by the squamous differentiation.

T1 hyperintensity may be observed within a deposit due to three contents: melanin, blood, and calcium.

- **Melanin-containing deposits**:   from melanoma (Figure 41 of Table 2).
- **Calcium-containing deposits**: Mucinous tumours of different origins (ovary, stomach, colon, pancreas, appendix, gallbladder, urachus) may calcify (Figure 42 of Table 2).
- **Blood-containing deposits**: Blood content is frequently found in peritoneal deposits from hypervascular tumours of different origins (for instance, clear cell and granulosa ovarian tumours) (Figure 43 of Table 2).

T2 hyperintensity can reflect different contents within deposits: myxoid, non-mineralized cartilage or mucin. It may also be due to keratin in the setting of a squamous differentiation.

- **Myxoid-containing deposits:** as in myxoid liposarcoma (Figure 44 of Table 2).
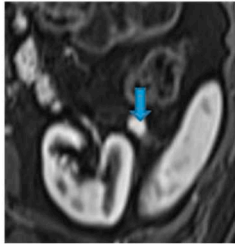
- **Non mineralized cartilage-containing deposits:** from chondrosarcoma (Figure 45 of Table 2).
- **Mucin-containing deposits:** from mucinous tumours arising on different organs, namely ovary, stomach, colon, pancreas, appendix, gallbladder and the urachus (Figure 46 of Table 2).
- **Keratin-containing deposits:** from tumours showing a squamous differentiation (Figure 47 of Table 2).

CT hyperdensity can be due to calcium (Figure 48 of Table 2) or blood content. Calcification may occur secondary to treatment.
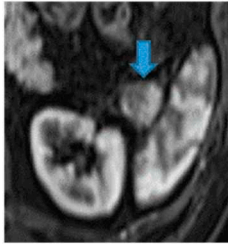
The vascular pattern of deposits also correlates with the characteristics of the primary tumour and may have an impact on the differential diagnosis (Table 3) depending on whether deposits are hyper (Figure 49 of Table 3) or hypovascular (Figure 50 of Table 3).

Table 3. Relation between vascular pattern of the deposits and differential diagnosis of possible primary tumours.	
Hypervascular deposits	**Hypovascular deposits**
Ovarian (clear cell, granulosa)	Mucinous tumours (ovary, stomach, colon, pancreas, appendix, gallbladder, urachus)
Breast carcinoma	Pancreas adenocarcinoma
Lung carcinoma	Liposarcoma (myxoid or undifferentiated)
Melanoma	
Sarcoma: - GIST -Leiomyosarcoma -Fibrous solitary tumour	
Renal cell carcinoma	
Neuroendocrine tumours	
Hepatocellular carcinoma	
Thyroid carcinoma	
Paraganglioma	
Choriocarcinoma	
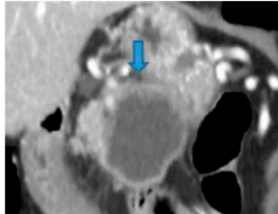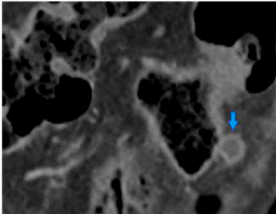
Figure 49. Axial CE portal phase FST1WI. PC from clear cell renal carcinoma: Note the hypervascular deposit adjacent to the spleen that was mistaken for an accessory spleen (**A**). Observe the growth on the follow-up CT (**B**).

Figure 50. Coronal MPR CE CT PC from pancreatic cystoadenocarcinoma: Observe the primary tumour (**A**) and its deposit within the sigmoid mesocolon (**B**). Notice the hypovascular resemblance between them.

6. Differential Diagnosis

It is worth underlining that in oncologic patients not all peritoneal abnormalities correspond to carcinomatosis and hence, PC needs to be differentiated from other neoplastic and non-neoplastic

conditions (inflammatory, infectious, and other types of benign causes, non-inflammatory and non-infectious) (Table 4). This may turn out to be a challenging task as imaging features often overlap.
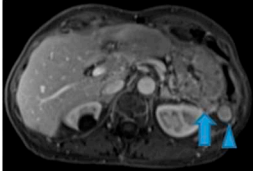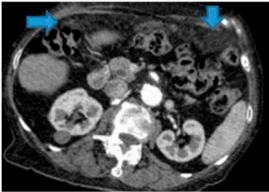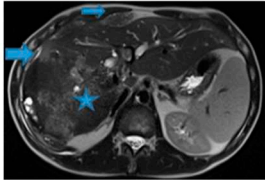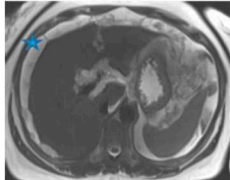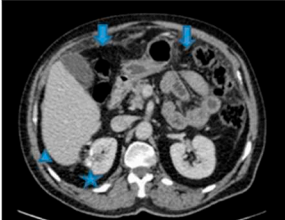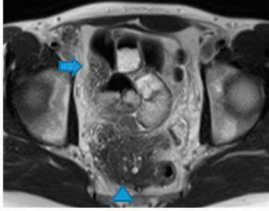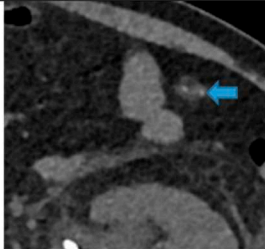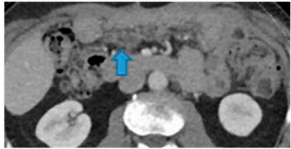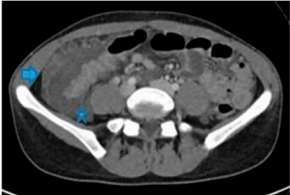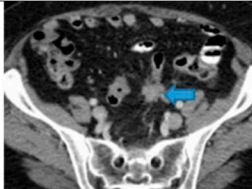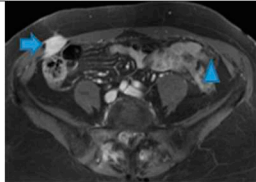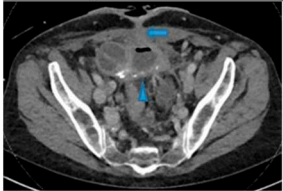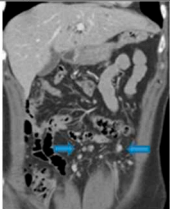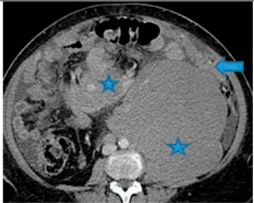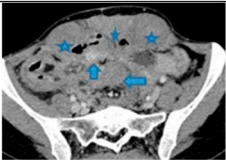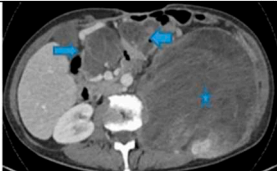
Table 4. Differential diagnosis

Inflammatory	Infectious	Benign non-inflammatory non-infectious	Malignant
Omental infarction	Peritoneal tuberculosis	Splenosis Accessory spleen	Primary peritoneal serous carcinoma
 Figure 51	 **Figure 56**	 **Figure 59**	 **Figure 65**
Peritoneal amyloidosis	Peritoneal echinococcosis	Bowel perforation	Pseudomyxoma peritoneal
 Figure 52	 **Figure 57**	 **Figure 60**	 **Figura 66**
Peritoneal sarcoidosis		Encapsulated omental fat necrosis	Peritoneal malignant mesothelioma
 Figure 53	 **Figure 58**	 **Figure 61**	 **Figure 67**
Familial Mediterranean fever		Endometriosis	Desmoplastic small round cell tumour
 Figure 54		 **Figure 62**	 **Figure 68**

Inflammatory	Infectious	Benign non-inflammatory non-infectious	Malignant
Encapsulated sclerosing peritonitis		Leiomyomatosis peritonealis	Peritoneal lymphomatosis
Figure 55		Figure 63	Figure 69
		Desmoid tumours	**Peritoneal sarcomatosis**
		Figure 64	Figure 70

Table 4. Differential diagnosis (continuation)

6.1. Inflammatory

6.1.1. Omental Infarction

Omental infarction is a rare cause of acute abdomen, usually self-limiting, that presents with non-specific symptoms. The right omentum is more commonly affected as it moves more freely, and its vascularization is longer and more tortuous. It can be primary or secondary to other processes such as tumour, hernia, and postoperative adhesions [27]. It is usually a straightforward diagnosis on CT: striking fat stranding of the infarcted omentum with minimal or no involvement of the adjacent bowel (this is the reason why the fat stranding is usually described as disproportionate) [28].

Omental infarction may mimic PC at a first glance, but the clinical setting and the inflamed aspect of the omental fat usually give away the diagnosis. The importance of the correct diagnosis on imaging relies on its conservative management unless it becomes superinfected.

Figure 51 of **Table 4**. Axial CE-CT. Patient with no known prior history, who presented with abdominal pain. Notice the salient fat stranding of the right omentum with mass effect on transverse colon but otherwise no involvement of the adjacent bowel. The diagnosis was omental infarction and it resolved within days.

6.1.2. Peritoneal Amyloidosis

Amyloidosis is a rare disease consisting of abnormal protein deposition throughout the body, which more frequently occurs in the gastrointestinal tract, in kidneys and in the heart. Peritoneal deposition is very rare and can mimic PC [29].

Two forms of peritoneal involvement have been described [30]: diffuse, in which the peritoneum is diffusely thickened and nodular, where mesenteric masses are the key finding. Calcifications may be found within the deposits.

Figure 52 of **Table 4).** Axial CE-CT. Patient with known cardiac amyloidosis. Observe the soft-tissue nodular-pattern infiltration within the omentum. Findings were stable compared to a CT from ten years prior. The peritoneal lesions were biopsied, and the histopathological exam concluded peritoneal amyloidosis.

6.1.3. Peritoneal Sarcoidosis

Sarcoidosis is a systemic granulomatous disease of unknown aetiology. The most common location is the lung [31]. Extrapulmonary involvement is found in 30% of all cases, the abdomen being the most frequent site and patients typically present with hepatosplenomegaly. Peritoneal involvement is a rare presentation, and the most frequent findings are ascites and peritoneal nodules. Peritoneal involvement is most frequently accompanied by a generalized disease that gives away the diagnosis, but the histological exam is necessary to confirm it [32].

Figure 53 of **Table 4**. Axial CE-CT. Patient on surveillance for a low-grade papillary renal cell carcinoma who underwent surgery five years ago (*). Note the omental infiltration (arrows) and the nodular thickening of the hepatic surface (arrowheads). PC was first suspected, though wearily, given its unlikeliness in the setting of a low-grade papillary renal cell carcinoma. A thorax CE-CT, not shown, revealed mediastinal adenopathies and peritoneal biopsy proved it to be a peritoneal sarcoidosis.

6.1.4. Familial Mediterranean Fever

It is a hereditary condition characterized by recurrent episodes of fever and systemic serosal inflammation, which occurs mainly in the abdomen. It affects especially patients of Mediterranean heritage. Imaging features are nonspecific, if it presents with ascites and peritonitis, it may strongly mimic PC [33]. The most fatal complication of FMF is amyloidosis and the chances of developing it are higher if untreated [34].

Figure 54 of **Table 4)**. Axial CE-CT. 25-year-old patient with no medical history presenting with abdominal discomfort. CT showed a peritoneal mass resembling an omental-cake (arrows) with ascites (*) and bilateral pleural effusion (not shown). A PC of unknown primary tumour was suspected. Her referring doctor later provided further clinical information: the patient suffered from recurrent inflammatory episodes. She responded to oral colchicine and was diagnosed with Familial Mediterranean fever.

6.1.5. Encapsulating Sclerosing Peritonitis

It is a rare but serious condition. It can be idiopathic or secondary, either to peritoneal dialysis or other causes, both benign such as surgery, peritonitis, cirrhosis, enteritis and malignant, such as pancreatic and renal adenocarcinoma [35]. It presents with recurrent episodes of bowel obstruction caused by a thickened and calcified peritoneal membrane that encircles the bowel [36].

Figure 55 of **Table 4**. Axial CE-CT. Patient with a known peritoneal pseudomyxoma treated with surgery and CHIP, who developed an encapsulating sclerosing peritonitis. Observe the clustered SB loops encircled by a thick calcified membrane (arrowhead). Also note an enterocutaneous fistula as a complication (arrow).

6.2. Infectious

6.2.1. Peritoneal Tuberculosis

Peritoneal tuberculosis may be a challenging entity to diagnose, given its insidious onset, its vague clinical presentation (abdominal pain and distention, weight loss and fever) and the difficult isolation of the agents (M. tuberculosis complex) [37].

It is important to achieve a prompt diagnosis as a delay in treatment may cause a worse outcome. Imaging classification includes three main types [38]:

- Wet (the most common), where the salient feature is ascites, either free or loculated, which may show high attenuation on CT due to high protein.
- Dry, where cellular content is predominant.
- Fibrotic-fixed, where the main features are fibrotic changes, causing clustered SB loops.
- An in-between state may also be found (Fibrotic-mixed).

The findings may overlap with PC but the presence of a smooth peritoneum with minimal thickening and pronounced enhancement suggests PT, whereas nodular implants and irregular

peritoneal thickening suggest PC.   Prominent mesenteric and retroperitoneal adenopathies may be seen in PT, which may present a necrotic centre and rim enhancement.

Figure 56 of **Table 4**. Axial CE-CT. Patient from Mali with a constitutional syndrome. CT showed multiple low density omental nodules (arrow) and retroperitoneal and mesenteric adenopathies (arrowhead). Multiple hypodense splenic lesions were also noted (fine arrow). There was loculated subhepatic ascites and mild free ascites (not shown). Thorax CT (not included here) also showed sternal lytic lesions with soft tissue components, mediastinal adenopathies and bilateral pleural effusion. Differential diagnosis included disseminated tuberculosis and PC of unknown origin. PCR-test of sample obtained by fine needle aspiration on an axillary adenopathy concluded disseminated tuberculosis (probably dry type as the cellular content is the salient feature).

6.2.2. Peritoneal Echinococcosis

It is a parasitic condition secondary to peritoneal seeding of Equinococcus larvae. The two main species of the Echinococcus tapeworm are: E. granulosus, the causal agent in cystic echinococcosis, also known as hydatid disease hosts and E. multilocularis, in alveolar echinococcosis [39]. Both domestic and wild canines are the definite hosts and humans are potentially involved as intermediate hosts [40]. In both entities, the initial infestation is localized to the liver.

E. granulosus hydatid cysts appear as well-defined thick-walled cystic lesions, with mural calcifications as a characteristic feature [41]. Peritoneal involvement generally results from rupture of hepatic or splenic cysts, with ascites and peritoneal enhancement as the main imaging features. Daughter cysts scattered throughout the peritoneal cavity may also be found.

On the other hand, hepatic alveolar echinococcosis usually appears as tumour-like infiltrative and partially calcified heterogeneous mass, with cystic and necrotic components. It may spread directly to the peritoneum, resulting in peritoneal lesions presenting the same imaging characteristics, that will inevitably mimic features of peritoneal carcinomatosis. The most salient feature is the infiltrative behaviour, with a tendency to invade adjacent structures. It is important to achieve an early diagnosis, as complete surgical excision is the only curative treatment [42].

Figure 57 and 58 of Table 4. Axial T2WI. Patient with no prior history who presented to the ER with abdominal pain. A rectal mass (arrow) was discovered along with a mass in the liver (*) and several peritoneal nodules (arrowheads). All the lesions showed the same heterogeneous signal intensity and infiltrative behaviour. The rectal mass was endoscopically biopsied and histology exam concluded it was an Echinococcus granulosus hepatic abscess with peritoneal dissemination.

6.3. Benign Non-Inflammatory/Non-Infectious

6.3.1. Splenosis/Accessory Spleen

These terms comprehend ectopic foci of splenic tissue that may be found throughout the abdominal cavity, differing in whether the cause is acquired (splenosis) or congenital (accessory spleen).

Splenosis is usually a consequence of spleen injury, either from trauma or surgery, resulting in splenic fragments that acquire vascular supply and that may grow. They may happen to seed on the liver, as the case shown in figure though most frequently in the left lobe, with a subcapsular location. Intrahepatic splenosis usually shows increased enhancement on the arterial phase and so it may be a potential pit fall for hepatocarcinoma, neuroendocrine metastases or adenoma [43–45]. Definitive diagnosis will be confirmed by a heat-denaturation red blood cell scintigraphy.

Accessory spleens will enhance as the spleen although this may be difficult to evaluate, due to their small size. As a rule, these nodules are well defined and homogeneous, whereas peritoneal deposits may tend to be more irregular and heterogeneous.

Figure 59 of Table 4. Axial CE portal phase FST1WI. Patient on follow up for ovarian carcinoma. Left subphrenic deposits (arrow) that were mistaken for accessory spleens (the patient had undergone tumour resection, which included a splenectomy). Note the accessory spleen adjacent to the deposits (arrowhead) and the distinct differences between them: deposits show irregular contours

and heterogeneous enhancement opposed to the smoothly outlined and homogeneously enhanced accessory spleen.

6.3.2. Foreign Body Bowel Perforation

Inflammatory-phlegmonous changes secondary to bowel perforation caused by a foreign body may mimic peritoneal carcinomatosis in oncologic patients.

Figure 60 of Table 4. Patient on follow up for a breast carcinoma. A suspiciously positive lesion within the transverse mesocolon was noted on PET-CT (not shown) and the report concluded possible PC, given the oncologic history. When the CT was reviewed, a calcified central elongated foreign body was identified (arrow). The diagnosis shifted to a colon perforation due to a fish bone and it resolved spontaneously.

6.3.3. Encapsulated Omental Fat Necrosis

Either spontaneous or secondary to inflammation or trauma, it is usually asymptomatic and its presentation on imaging depends on the time of evolution. On CT, if acute, it appears as an omental or mesenteric focal fat stranding that may show a discrete mass effect on the adjacent organs; over time it shrinks and becomes well defined and peripherally calcified. Initially it may mimic a liposarcoma and when it becomes fibrotic (usually it shows heterogeneous low signal intensity on T1 and T2WI and may enhance slightly) it can be misdiagnosed as a deposit, especially in oncologic patients. Clinical history and previous imaging examinations are essential to achieve a correct diagnosis.

Figure 61 of Table 4. Axial NE-CT. Encapsulated omental fat necrosis (arrow) that was misdiagnosed as a peritoneal deposit on an ovarian malignancy follow-up. When compared to previous CT, it was stable and punctate calcifications within it were noticed (arrow).

6.3.4. Endometriosis

It is a benign condition characterized by the implantation of endometrial tissue outside the uterine cavity. Peritoneal endometriosis is usually accompanied by other imaging findings that suggest the diagnosis; however, peritoneal involvement may appear as the sole finding. Endometriotic deposits will likely show areas of high signal intensity on T1WI due to blood content and/or low signal intensity on T2WI due to fibrosis.

Figure 62 of Table 4. Axial CE CT. 40-year-old female patient with no prior history who was discovered to have a mesosigmoid spiculated lesion on a check-up for abdominal pain. The differential diagnosis included a peritoneal deposit of an unknown primary tumour or a desmoplastic reaction of an unknown neuroendocrine tumour. The biopsy revealed an endometriotic peritoneal deposit.

6.3.5. Peritoneal Leiomyomatosis

Rare condition that occurs in women of reproductive age, characterized by the development of multiple leiomyomas within the peritoneum. Potential risk factors are increased levels of endogenous/exogenous oestrogens [46] and prior laparoscopic myomectomy [47].

Malignant transformation is a rare complication [48]. Peritoneal leiomyomas are observed as iso-hypodense nodules on CT with a muscle-like signal intensity on MR and strong homogeneous enhancement, which turns heterogeneous (due to necrosis and haemorrhage) in the event of malignant transformation. This entity may mimic a PC of unknown origin. Definitive diagnosis is made histopathologically.

Figure 63 of Table 4. CE-CT coronal MPR. 45-year-old patient with no known primary tumour. On a pelvic MR for uterine fibroids, peritoneal nodules were identified, and an abdominal MR was performed. Multiple hyperenhancing omental nodules were noted (arrows) and she was diagnosed with a PC of unknown origin. She underwent an explorative laparoscopy with partial omentectomy:

it turned out to be a disseminated peritoneal leiomyomatosis that responded well to hormonal treatment.

6.3.6. Desmoid Tumours

Desmoid tumours (DT) belong to a heterogeneous group of locally aggressive fibromatosis, though non-metastasising, that may arise throughout the body, most commonly extra-abdominally. In 30% of the patients there is an association with familial adenomatous polyposis and in this setting, tumours are most frequently multiple and intra-abdominal (80%, compared to 5% of intra-abdominal sporadic DT) [49].

There is also an association with pregnancy and prior trauma, or surgery have been described as possible risk factors [50].   In the abdomen, they are mostly mesenteric, although pregnancy-associated DT usually occur within the abdominal wall [51].

DT are soft tissue masses that may show either well-demarcated or ill-defined margins that extend into the adjacent mesenteric fat. They are usually isodense to muscle, their signal intensity on MR depending on the predominant content (myxoid, cellular or fibrosis). Enhancement ranges from moderate to intense. As infiltrating mesenteric soft tissue masses, they can mimic PC.

Figure 64 of Table 4. Axial CE-CT. Young female presenting multiple desmoid tumours in the setting of Gardner´s syndrome: mesenteric (arrows) and within the anterior abdominal wall (*).

6.4. Malignant

6.4.1. Primary Peritoneal Serous Carcinoma

It occurs in women, predominantly postmenopausal, and is a challenging diagnosis as it resembles advanced epithelial ovarian carcinoma (AEOC), both in imaging and in the histological exam. It occurs less frequently that AEOC and has a worse prognosis [52]. The distinguishing features are the sparing of the ovaries, or the disproportionate burden of extra-ovarian disease compared to the ovarian involvement [53].

Figure 65 of Table 4. Axial CE-CT. Young female patient who presented with bloating. Note the extensive peritoneal disease (arrow), partly calcified. Calcifications suggest a mucinous tumour and more frequently, a serous ovarian adenocarcinoma, but the ovaries (not shown) appeared to be almost normal. Thus, a primary peritoneal serous carcinoma was the first hypothesis and was biopsy proven following a laparoscopic exam.

6.4.2. Pseudomyxoma Peritoneal

It is a clinical term that refers to a syndrome characterized by the presence of mucinous loculated ascites within the peritoneum [54].

These mucinous septated collections disseminate along the peritoneal surface and their mass effect causes a scalloped appearance of adjacent organs. Pseudomyxoma cells lack adherence molecules on their surface so they will spread by a redistribution phenomenon, which means they follow the current of the intraperitoneal fluid and tend to accumulate at the gravity dependent and resorption sites described at the beginning of this review [55]. Thus, the mobile small bowel will be initially spared, thanks to its continuous peristaltic movement.

This entity has been classically associated with a perforated epithelial neoplasm of the appendix, although less frequently, it can originate from mucinous tumours arising from other organs [56].   It should be distinguished from mucinous peritoneal carcinomatosis, as they are conditions that differ histologically, on imaging findings and prognosis [57].

Figure 66 of Table 4. Axial T2WI. Observe loculated mucin (*) in this patient with a known PP, notice the characteristic scalloped appearance of the coated organs.

6.4.3. Peritoneal Malignant Mesothelioma (PMM)

This very rare and fatal primary malignancy of the peritoneum shows features that overlap those of PC, thus it is difficult to distinguish these entities on imaging alone. The link with asbestos exposure is weaker than in pleural mesothelioma but it remains its best-defined risk factor [58]: a history of asbestos exposure or the presence of pleural plaques can be helpful for differentiating PMM from PC.

Figure 67 of Table 4. Axial CE-CT. Note deposits within the mesentery in this patient with a known PMM. It is difficult to distinguish PC from PMM on imaging alone. However, an asbestos exposure history or the presence of pleural plaques as it was the case there (not shown) could be helpful for differentiating PMM from PC.

6.4.4. Desmoplastic Small Round Cell Tumour (DSRCT)

Rare mesenchymal malignancy that arises from peritoneal surfaces, as multiple soft tissue masses. It occurs most frequently in young male patients. Imaging features overlap with other peritoneal malignant tumours. Calcification may occur on 30% of the cases [59].

Figure 68 of Table 4. Axial CE portal phase FST1WI. 20-year-old male patient with no medical record who presented with a palpable abdominal mass. Observe the mass within the anterior parietal peritoneum (arrows) with invasion of the abdominal wall muscles. Also notice the omental infiltration (arrowhead). The histological exam proved it was a desmoplastic small round cell tumor (DSRCT).

6.4.5. Peritoneal Lymphomatosis and 6.4.6 Peritoneal Sarcomatosis

As described at the beginning of this review, the term peritoneal carcinomatosis is used when caused by epithelial cells. The peritoneum may also be the soil of malignant non-epithelial cellular lines: mesenchymal or lymphoid, thus referring to sarcomatosis and lymphomatosis respectively [9].

In the setting of an unknown primary tumour, the differential diagnosis should always include the possibility of another cell line being the origin of the peritoneal deposits.

Peritoneal lymphomatosis (PL) is a rare condition but important to suspect, as it responds favorably to chemotherapy. It is uncommon, as the peritoneum lacks lymphoid tissue, and the underlying mechanism is unknown. It is associated most frequently to diffuse large B-cell lymphoma, though it can occur in many subtypes [60].

Imaging features include homogeneous soft tissue diffuse infiltration of peritoneal leaves [9], associated with prominent retroperitoneal lymph nodes [61] and bulky mesenteric lymph nodes that surround the mesenteric vessels and the perivascular fat on both sides (sandwich sign) [62].   In presence of lymph nodes, the diagnosis is easier, as the burden of the nodal disease is usually disproportionate to the peritoneal disease and its distribution is more diffuse than in PC, where lymph nodes are usually located adjacent to the primary tumour [63].

Ascites, which can be massive in PC, is rather mild in PL and hepatosplenomegaly occurs more frequently.

Isolated peritoneal disease with no bowel or lymph node involvement is rare [64].

Bowel obstruction is uncommon, even in extensive lymphomatous infiltration of small bowel, due to its lack of desmoplastic reaction [65].

Figure 69 of Table 4. Axial CE-CT. Follicular NH lymphoma. Note the omental-cake (arrow), suspicious for PC. Nevertheless, the presence of coexisting bulky retroperitoneal and mesenteric adenopathies (*) are imaging features that favour PL over PC.

Peritoneal sarcomatosis (PS) is defined as a disseminated intraperitoneal spread either from an intra-abdominal primary sarcoma or from extremity sarcomas [66]. Sarcomatous peritoneal deposits tend to be larger, more hypervascular and heterogeneous (Table 2) than in PC. In addition, lymph node involvement is rare. Ascites is variable [67] and hemoperitoneum may occur more frequently than in PC [68].

Bowel obstruction and hydronephrosis tend to be more common in PC [68].

Despite these differences, diagnosis of peritoneal lymphomatosis/sarcomatosis based on imaging can be difficult to achieve given that carcinomatosis is much more frequent, thus, the diagnosis should be confirmed by histology.

Figure 70 of Table 4. Axial CE portal phase FST1WI. Sarcomatosis from retroperitoneal liposarcoma. Patient who underwent surgery for the primary tumour and who presents with a relapse showing a left retroperitoneal mass (*) and mesenteric deposits (arrows).

7. Conclusions

To correctly diagnose PC, a systematic approach of the abdominal cavity is highly recommended. The knowledge of peritoneal anatomy and peritoneal fluid flow characteristics will substantially contribute to understanding where to look for deposits and which is their appearance on cross section imaging.

Indeed, at CT and MR, features of peritoneal deposits and their behaviour on contrast-enhanced cross-section images are related to the histologic characteristics of the primary tumour. Therefore, in the event of peritoneal carcinomatosis with unknown primary tumour, signal intensity/density characteristics of the peritoneal deposits together with their vascular properties may be helpful in the identification of the primary tumour.

Moreover, it can occur that the sole presenting sign of peritoneal carcinomatosis are intra-abdominal complications such bowel obstruction or ureterohydronephrosis which should be considered suspicious in oncologic patients, even in absence of clear radiological evidence of peritoneal deposits.

Furthermore, there are several benign and malignant peritoneal conditions that may mimic peritoneal carcinomatosis. Thus, even in oncologic patients, it is important to consider these conditions in the differential diagnosis with peritoneal carcinomatosis. However, relying solely on imaging it remains difficult to make the differential diagnosis since the imaging features overlap between benign/other malignant conditions.

References

1. Flanagan, M.; Solon, J. Peritoneal metastases from extra-abdominal cancer - A population-based study. Eur J Surg Oncol. 2018, 44(11), 1811-1817. doi: 10.1016/j.ejso.2018.07.049.
2. Desai, J.P.; Moustarah, F. Peritoneal Metastasis. In: StatPearls [Internet]. Treasure Island (FL): StatPearls Publishing, 2022.
3. González-Moreno, S.; González-Bayón, L. Imaging of peritoneal carcinomatosis. Cancer J Sudbury Mass. 2009, 15(3), 184–9.
4. Patel, C.M.; Sahdev; A. CT, MRI and PET imaging in peritoneal malignancy. Cancer Imaging. 2011, 11(1), 123–39.
5. Van 't Sant, I.; Engbersen, M.P. Diagnostic performance of imaging for the detection of peritoneal metastases: a meta-analysis. Eur Radiol. 2020, 30(6), 3101–12.
6. Cianci, R.; Delli Pizzi, A. Magnetic Resonance Assessment of Peritoneal Carcinomatosis: Is There a True Benefit from Diffusion-Weighted Imaging? Curr Probl Diagn Radiol. 2020, 49, 392–7.
7. Low, R.N. Magnetic Resonance Imaging in the Oncology Patient: Evaluation of the Extrahepatic Abdomen. Semin Ultrasound CT MRI. 2005, 26(4), 224–36.
8. Kim, S.J.; Lee, S.W. Diagnostic accuracy of (18)F-FDG PET/CT for detection of peritoneal carcinomatosis; a systematic review and meta-analysis. Br J Radiol, 2018, 91, 20170519
9. Cabral, F.C.; Krajewski, K.M. Peritoneal lymphomatosis: CT and PET/CT findings and how to differentiate between carcinomatosis and sarcomatosis. Cancer Imaging. 2013, 13(2), 162-70. doi: 10.1102/1470-7330.2013.0018.
10. Low, R.N. MR imaging of the peritoneal spread of malignancy. Abdom Imaging. 2007, 32, 267–83. doi: 10.1007/s00261-007-9210-8
11. Tirkes, T.; Sandrasegaran, K. Peritoneal and retroperitoneal anatomy and its relevance for crosssectional imaging. Radiographics. 2012, 32(2), 437-51.
12. Gore, R.M.; Levine, L.S. Textbook of gastrointestinal radiology. 3rd ed.; Saunders, 2007; pp. 2071-97.
13. Meyers, M.A.; Oliphant, M. The peritoneal ligaments and mesenteries: pathways of intraabdominal spread of disease. Radiology. 1987, 163, 593–604.
14. Nougaret, S.; Addley, H.C. Ovarian carcinomatosis: how the radiologist can help plan the surgical approach. Radiographics. 2012, 32(6), 1775-800.

15.   Akin, O.; Sala, E. Perihepatic metastases from ovarian cancer: sensitivity and specificity of CT for the detection of metastases with and those without liver parenchymal invasion. Radiology. 2008, 248(2), 511–517.

16.   Winston, C.B.; Hadar, O. Metastatic lobular carcinoma of the breast: patterns of spread in the chest, abdomen, and pelvis on CT. AJR Am J Roentgenol. 2000, 175(3), 795-800. doi: 10.2214/ajr.175.3.1750795.

17.   Healy, J.C.; Reznek, R.H. The peritoneum, mesenteries and omenta: normal anatomy and pathological processes. Eur Radiol. 1998, 8(6), 886-900. doi: 10.1007/s003300050485. PMID: 9683690.

18.   Xu, Y.; Yang, J. MRI for discriminating metastatic ovarian tumors from primary epithelial ovarian cancers. J Ovarian Res, 2015, 8, 61. doi: 10.1186/s13048-015-0188-5.

19.   Zulfiqar, M.; Koen, J. Krukenberg Tumors: Update on Imaging and Clinical Features. AJR Am J Roentgenol. 2020, 215(4), 1020-1029. doi: 10.2214/AJR.19.22184.

20.   Kim, S.H.; Kim, W.H. CT and MR findings of Krukenberg tumors: comparison with primary ovarian tumors. Journal of Computer Assisted Tomography. 1996, 20(3), 393–8.

21.   Saif, M.W.; Siddiqui, I.A. Management of ascites due to gastrointestinal malignancy. Ann Saudi Med. 2009, 29(5), 369-377.

22.   Chang, D.K.; Kim, J.W. Clinical significance of CT-defined minimal ascites in patients with gastric cancer. World J Gastroenterol. 2005, 11(42), 6587.

23.   Meyers, M.A. Intraperitoneal seeding: pathways of spread and localization. In: Meyers' dynamic radiology of the abdomen, 6th ed.; Meyers, M.A., Charnsangavej, C.; Springer, New York, 2000, pp. 69-105.

24.   Coakley, F.V.; Hricak, H. Imaging of peritoneal and mesenteric disease: key concepts for the clinical radiologist. Clin Radiol. 1999, 54(9), 563–574.

25.   Feldman, G.B.; Knapp, R.C. Lymphatic drainage of the peritoneal cavity and its significance in ovarian cancer. Am J Obstet Gynecol. 1974, 119, 991–994.

26.   Seltzer, S.E. Analysis of the tethered-bowel sign on abdominal CT as a predictor of malignant ascites. Gastrointest Radiol. 1987, 12, 245–249. doi : 10.1007/BF01885152

27.   Leitner, M.J.; Jordan, C.G. Torsion, infarction and hemorrhage of the omentum as a cause of acute abdominal distress. Ann Surg. 1952, 135(1), 103-10.

28.   Pereira, J.M.; Sirlin, C.B. Disproportionate fat stranding: a helpful CT sign in patients with acute abdominal pain. Radiographics. 2004, 24(3), 703-715. Preprints (www.preprints.org) | NOT PEER-REVIEWED | Posted: 9 May 2023 doi:10.20944/preprints202305.0576.v1

29.   Pickhardt, P.J.; Bhalla S. Unusual nonneoplastic peritoneal and subperitoneal conditions: CT findings. Radiographics. 2005, 25, 719–30.

30.   Kim, M.S.; Ryu J.A. Amyloidosis of the mesentery and small intestine presenting as a mesenteric haematoma. Br J Radiol. 2008, 81, e1–3.

31.   Iannuzzi, M.C.; Rybicki, B.A. Sarcoidosis. New Engl J Med. 2007, 357, 2153–65.

32.   Gezer, N.S.; Basara, I. Abdominal sarcoidosis: cross-sectional imaging findings. Diagn Interv Radiol. 2015, 21, 111–7.

33.   Zissin, R.; Rathaus, V. CT findings in patients with familial Mediterranean fever during an acute abdominal attack. Br J Radiol. 2003, 76(901), 22-5. doi: 10.1259/bjr/32051823.

34.   Bhatt, H.; Cascella, M. Familial Mediterranean Fever. In: StatPearls [Internet]. Treasure Island (FL): StatPearls Publishing, 2022.

35.   Manphool, S.; Satheesh, K. Encapsulating peritoneal sclerosis: the abdominal cocoon. Radiographics. 2019, 39(1), 62-77.

36.   Singhal, M.; Krishna S. Encapsulating Peritoneal Sclerosis: The Abdominal Cocoon. Radiographics. 2019, 39(1), 62-77. doi: 10.1148/rg.2019180108.

37.   Uygur-Bayramicli, O.; Dabak, G. A clinical dilemma: abdominal tuberculosis. World J Gastroenterol. 2003, 9(5), 1098-101. doi: 10.3748/wjg.v9.i5.1098.

38.   Burrill, J.; Williams, C.J. Tuberculosis: a radiologic review. Radiographics. 2007, 27(5), 1255-73. doi: 10.1148/rg.275065176.

39.   Pedrosa, I.; Saíz, A. Hydatid disease: radiologic and pathologic features and complications. Radiographics. 2000, 20(3), 795-817. doi: 10.1148/radiographics.20.3.g00ma06795.

40.   Moro, P.; Schantz, P.M. Echinococcosis: a review. Int J Infect Dis. 2009, 13(2), 125–33. doi:10.1016/j.ijid.2008.03.037

41.   Zalaquett, E.; Menias, C. Imaging of hydatid disease with a focus on extrahepatic involvement. Radiographics. 2007, 37, 901-923.

42.   McManus, D.P.; Zhang, W. Echinococcosis. Lancet. 2003, 362(9392), 1295–1304.

43.   Sato, N.; Abe, T. Intrahepatic splenosis in a chronic hepatitis C patient with no history of splenic trauma mimicking hepatocellular carcinoma. Am J Case Rep. 2014, 15, 416-20.

44.   Leong, C.W; Menon, T. Post-Traumatic Intrahepatic Splenosis Mimicking a Neuroendocrine Tumour. BMJ Case Rep. 2013.

45.   Gruen, D.R.; Gollub, M. Intrahepatic splenosis mimicking hepatic adenoma. AJR Am J Roentgenol. 1997, 168, 725-726.

46.   Drake, A.; Dhundee, J. Disseminated leiomyomatosis peritonealis in association with oestrogen secreting ovarian fibrothecoma. BJOG. 2001, 108(6), 661-4. doi: 10.1111/j.1471-0528.2001.00132.x.

47.   Kumar, S.; Sharma, J.B. Disseminated peritoneal leiomyomatosis: an unusual complication of laparoscopic myomectomy. Arch Gynecol Obstet. 2008, 278(1), 93-5. doi: 10.1007/s00404-007-0536-9. Epub 2008 Jan 12. PMID: 18193441.

48.   Surmacki, P.; Sporny, S. Disseminated peritoneal leiomyomatosis coexisting with leiomyoma of the uterine body. Arch Gynecol Obstet. 2006, 273(5), 301-3. doi: 10.1007/s00404-005-0086-y.

49.   Sinha, A.; Hansmann, A. Imaging assessment of desmoid tumours in familial adenomatous polyposis: is state-of-the-art 1.5 T MRI better than 64-MDCT? Br J Radiol. 2012, 85(1015), e254–261

50.   Brooks, A.P., Reznek R.H. CT appearances of desmoid tumours in familial adenomatous polyposis: further observations. Clin Radiol. 1994, 49, 601–607

51.   Robinson, W.A.; McMillan C. Desmoid tumors in pregnant and postpartum women. Cancers (Basel). 2012, 4(1), 184–192

52.   Li, X.; Yang, Q. Differences between primary peritoneal serous carcinoma and advanced serous ovarian carcinoma: a study based on the SEER database. J Ovarian Res. 2021, 14, 40 (2021). doi: 10.1186/s13048-021-00788-y

53.   Morita, H.; Aoki, J. Serous surface papillary carcinoma of the peritoneum: clinical, radiologic, and pathologic findings in 11 patients. American Journal of Roentgenology. 2004, 183(4), 923-928.

54.   Diop, A.D.; Fontarensky, M. CT imaging of peritoneal carcinomatosis and its mimics. Diagn Interv Imaging. 2014, 95(9), 861-72. doi: 10.1016/j.diii.2014.02.009.

55.   Sugarbaker, P.H. Pseudomyxoma peritonei. A cancer whose biology is characterized by a redistribution phenomenon. Ann Surg. 1994, 219(2), 109-11. doi: 10.1097/00000658-199402000-00001.

56.   Mittal, R.; Chandramohan, A. Pseudomyxoma peritonei: natural history and treatment. Int J Hyperthermia. 2017, 33(5), 511-519.

57.   Ronnett, B.M.; Yan H. Patients with pseudomyxoma peritonei associated with disseminated peritoneal adenomucinosis have a significantly more favorable prognosis than patients with peritoneal mucinous carcinomatosis. Cancer. 2001, 92(1), 85-91. doi: 10.1002/1097-0142(20010701)92:1<85::aidcncr1295>3.0.co;2-r. Preprints (www.preprints.org) | NOT PEER-REVIEWED | Posted: 9 May 2023 doi:10.20944/preprints202305.0576.v1

58.   Broeckx, G.; Pauwels P. Malignant peritoneal mesothelioma: a review. Transl Lung Cancer Res. 2018, 7(5), 537-542. doi: 10.21037/tlcr.2018.10.04.

59.   Chen, J.; Wu, Z. Intra-abdominal desmoplastic small round cell tumors: CT and FDG-PET/CT findings with histopathological association. Oncol Lett. 2016, 11, 3298-3302.

60.   Yoo, E.; Kim, J.H. Greater and lesser omenta: normal anatomy and pathologic processes. Radiographics. 2007, 27(3), 707-20. doi: 10.1148/rg.273065085.

61.   Karaosmanoglu D, Karcaaltincaba M, Oguz B, Akata D, Ozmen M, Akhan O. CT findings of lymphoma with peritoneal, omental and mesenteric involvement: peritoneal lymphomatosis. Eur J Radiol. 2009, 71(2), 313-7. doi: 10.1016/j.ejrad.2008.04.012.

62.   Hardy, S.M. Signs in imaging: the sandwich sign. Radiology. 2003, 226(3), 651–652.

63.   Kim, Y.; Cho, O. Peritoneal lymphomatosis: CT findings. Abdom Imaging. 1998, 23, 87–90. doi: 10.1007/s002619900292.

64.   Wong, S.; Sanchez, T.R.S. Diffuse peritoneal lymphomatosis: atypical presentation of Burkitt lymphoma. Pediatric radiology. 2009, 39, 274-276.

65.   Balthazar, E.J.; Noordhoorn, M. CT of small-bowel lymphoma in immunocompetent patients and patients with AIDS: comparison of findings. AJR Am J Roentgenol. 1997, 168(3), 675-680.

66.   Tamara, N.O.; Jyothi, P. Peritoneal sarcomatosis versus peritoneal carcinomatosis: imaging findings at MDCT. AJR Am J Roentgenol. 2010, 195(3), W229-35.

67.   Bilimoria, M.M.; Holtz, D.J. Tumor volume as a prognostic factor for sarcomatosis. Cancer. 2002, 94(9), 2441-6. doi: 10.1002/cncr.10504.

68.   Oei, T.N.; Jagannathan, J.P. Peritoneal sarcomatosis versus peritoneal carcinomatosis: imaging findings at MDCT. AJR Am J Roentgenol. 2010, 195(3), W229-35.